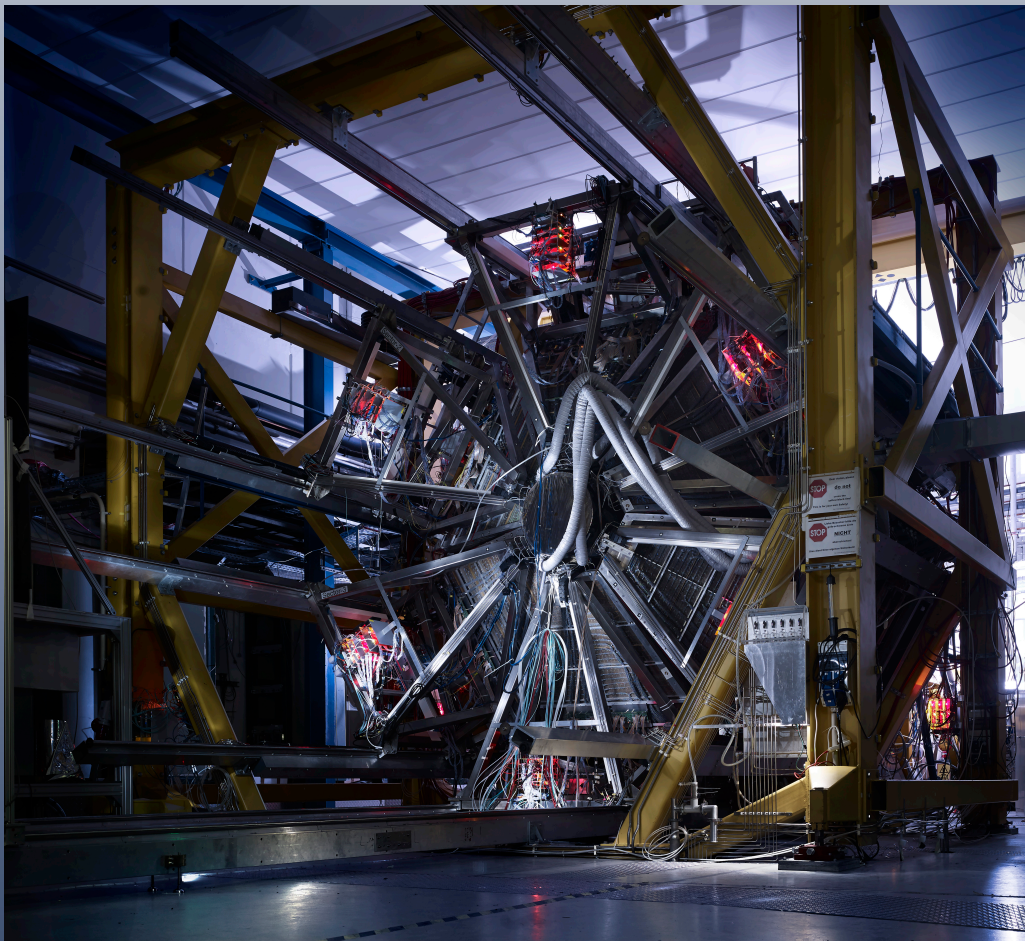


π - QCD

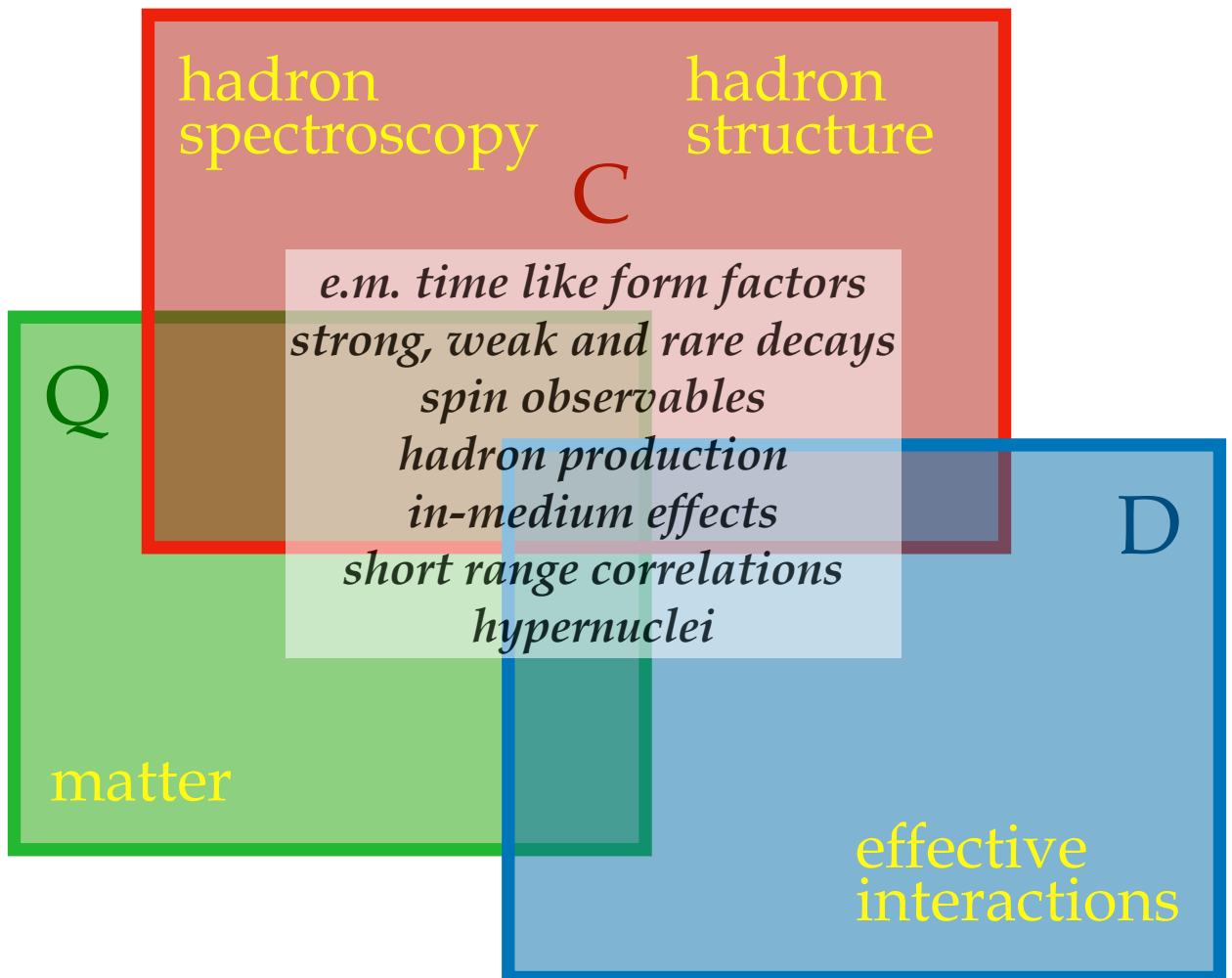
The HADES Collaboration



Proposal for Experiments at the
GSI Pion Beam Facility

December 2024
Version 0.1

π - QCD



boosting the understanding of
non-perturbative QCD
by combining pion beams with HADES
and involving three pillars

Disclaimer

This document outlines potential research topics to be explored using the secondary pion beam at GSI in combination with HADES. Its main objective is to present a comprehensive, strong-QCD-inspired program that addresses key questions across the heavy-ion, nuclear, and hadron physics communities. Please note that the content is 'work-in-progress' and will evolve as the supporting community grows and advances this initiative, laying the foundation for a lasting and innovative experimental program.

Abstract

We propose to investigate the dynamics of hadronic matter in the strong QCD regime using the pion-beam facility at GSI in conjunction with HADES. This program will study hadron physics through elementary pion-nucleon interactions up to $\sqrt{s} \approx 2.35$ GeV, bridging cold matter research with detailed analyses of exclusive reactions. Our goals include exploring baryon resonance formation and their electromagnetic structures up to the third resonance region, complementing photo-production experiments (e.g., ELSA) and enhancing understanding of emissivity in dense, hot hadronic matter. Key topics include examining baryon couplings to mesons and virtual photons, analyzing hyperon weak decays in exclusive reactions, and using Partial Wave Analyses with differential cross sections and polarization observables to achieve unprecedented precision in baryon-meson coupling data (ρN , ωN). Furthermore, e^+e^- production measurements off nucleons will provide insight into the electromagnetic transition form factors of baryons in the time-like region, revealing the role of vector mesons (ρ , ω). Reactions on nuclear targets allow for detailed studies of hadron properties, including vector-meson line shapes and strengths in cold nuclear matter. These measurements provide a critical reference between elementary π -nucleon interactions and the complex hot and dense environment in $A + A$ collisions. This research also has broader implications. It will contribute to the modeling of neutrino-nucleus interactions, facilitate unprecedented investigations into hypernuclei formation, and enhance our understanding of strong interaction dynamics across different energy regimes.

Contents

1	Introduction	6
2	<i>Q</i>: Cold matter	10
2.1	Introduction	10
2.2	In-medium vector-meson properties	11
2.3	Production and propagation of strangeness	11
2.4	Intermediate reference for heavy-ion data	12
2.5	Input for neutrino-nucleus reaction modeling	12
3	<i>C</i>: Hadron spectroscopy, structure, and exotics	14
3.1	Introduction	14
3.2	Baryon-meson couplings	14
3.3	Electromagnetic couplings	17
3.4	Exotic mesons	20
3.5	Rare eta meson decays	22
4	<i>D</i>: Effective interactions	24
4.1	Introduction	24
4.2	Hyperon polarization	24
4.3	Hypernuclei formation	25
4.4	Hyperon-meson interaction	26
5	Experimental set-up	28
5.1	The (upgraded) HADES facility	28
5.2	The GSI pion-beam facility	28
6	Submitted proposals GPAC 2025	35
7	Letters of support	49
8	The HADES Collaboration	57

1 Introduction

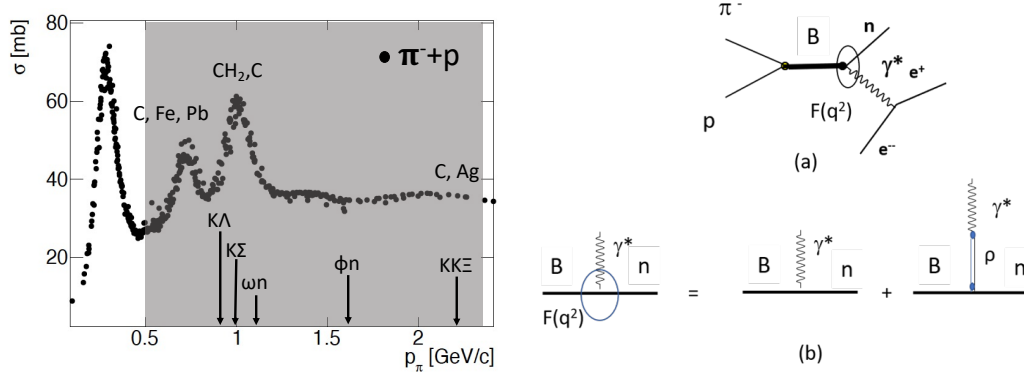


Figure 1: Left: $\pi^- + p$ cross sections (black dots). The black arrows indicate the thresholds for various hadronic final states. The gray shaded area corresponds to the momentum range covered by this proposal, the targets in the upper part mark the regions, in which they are used. Right: (a) Sketch of a time-like electromagnetic baryon transition in the $\pi^- + p$ reaction at a given four-momentum transfer $q^2 = M_{ee}^2$. (b) illustration of the two-component form factor model, consisting of a point-like photon coupling and an electromagnetic interaction mediated by vector mesons, according to the Vector Dominance Model (VMD).

Pion-matter interactions as tool for a collaborative QCD program

Pion-nucleon scattering has been fundamental to understanding nuclear binding forces, with pions serving as the (pseudo) Goldstone bosons of SU(2) flavor symmetry. The πN system is a well-established probe of strong QCD dynamics, attracting significant experimental and theoretical interest. Experimentally, pion-induced processes are relatively straightforward to interpret compared to, for example, nucleon-nucleon scattering. With a baryon number of one, these interactions typically produce two or three particles in the final state, facilitating rigorous partial-wave analyses (PWA) and allowing for high detection efficiencies that support the reconstruction of complete event topologies. Compared to complementary photo-production experiments, πN cross sections are substantially larger, enabling high-precision measurements within shorter beam times, making them an efficient tool for advancing our understanding of hadron dynamics.

A common interest in the nuclear, hadron, and heavy-ion physics communities has evolved towards understanding strong QCD guided by “SU(3) flavored systems”, addressing, *f.e.*, the role of strangeness in dense baryonic matter, such as expected to occur in the core of neutron stars. The program proposed in this document has the ambition to provide valuable data in this context by exploiting pion-beam experiment on proton and nuclear targets in the pion momentum 0.5-2.5 GeV/c see Fig. 1, Left (a). The program makes use of the unique combination of an intense pion beam ($10^6/s$) and the versatile HADES setup, which provides extensive phase-space coverage, precise momentum determination, state-of-the-art di-lepton detection, excellent particle identification, and photon detection capabilities via its newly completed electromagnetic calorimeter. These features enable precision measurements of a wide range of observables, including differential cross sections, branching fractions, time-like electromagnetic transition form factors, spin-density matrix elements, and the self-polarization of hyperons, for various reaction channels below and above the hyperon-production threshold.

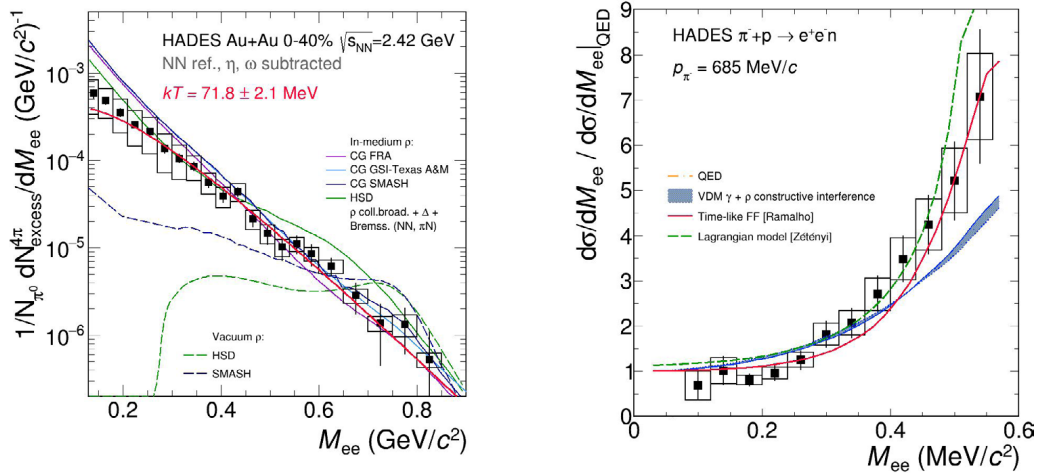


Figure 2: Left: Dilepton excess yield in the low invariant mass region identified as the modified ρ -spectral function. Different theoretical calculations are compared to the data measured by HADES in Au+Au collisions at 2.42 GeV [1]. Right: Invariant mass of pairs from $N^* \rightarrow N\gamma^* \rightarrow Ne^+e^-$ normalized by QED prediction for point-like transitions [2]. Figure taken from the NuPECC long-range plan 2024.

In studies of cold matter, the use of the πA initial state offers several key advantages compared to other probes, such as pA reactions. Most prominently, its kinematics allows to produce short-lived hadrons, such as the ω vector meson, with relatively small momenta with the recoil nucleus. This provides promising sensitivity for investigating in-medium effects, e.g. line shape and line strength measurements of vector-mesons, which are expected to manifest at low momenta. Secondly, pion-induced reactions are superior to the previously studied proton- and photon-induced reactions. Due to the large πN inelastic cross section, hadron production occurs close to the upstream surface of the nucleus, leading on average to a longer path of the produced hadrons inside the nuclear matter. Additionally, the high production cross-section of hyperons in π -induced reactions makes it particularly well-suited for the abundant formation of hypernuclei. Pion-induced cold matter studies also yield data that are crucial for testing and refining transport models. The significance of such datasets has been highlighted by neutrino experiments, such as T2K and DUNE, which depend on accurate particle production cross sections for reconstructing the energy of neutrinos in their detectors.

Pion beams at GSI: a proven success story

The physics potential of pion-induced reactions combined with HADES, particularly for cross-community applications, has been unequivocally demonstrated in previous studies. A notable example is the investigation of the $N^*(1520) \rightarrow Ne^+e^-$ electromagnetic transition form factor (emTFF) in $\pi^-p \rightarrow Ne^+e^-$ at a center-of-mass energy of $\sqrt{s} = 1.5$ GeV. The q^2 dependence of the emTFF, together with a partial-wave analysis of simultaneously reconstructed $\pi^-p \rightarrow \pi^+\pi^-n$ data, provided detailed insights into the validity of vector-meson dominance and the role of pion clouds. This information is crucial for understanding e^+e^- mass spectra in $A+A$ reactions, especially in the context of the ρ contribution melting in baryon-dense environments as illustrated in Fig. 2.

The proposed program exploiting the pion-beam and HADES facilities enables detailed investigations of both hadronic and electromagnetic properties of matter. The versatility

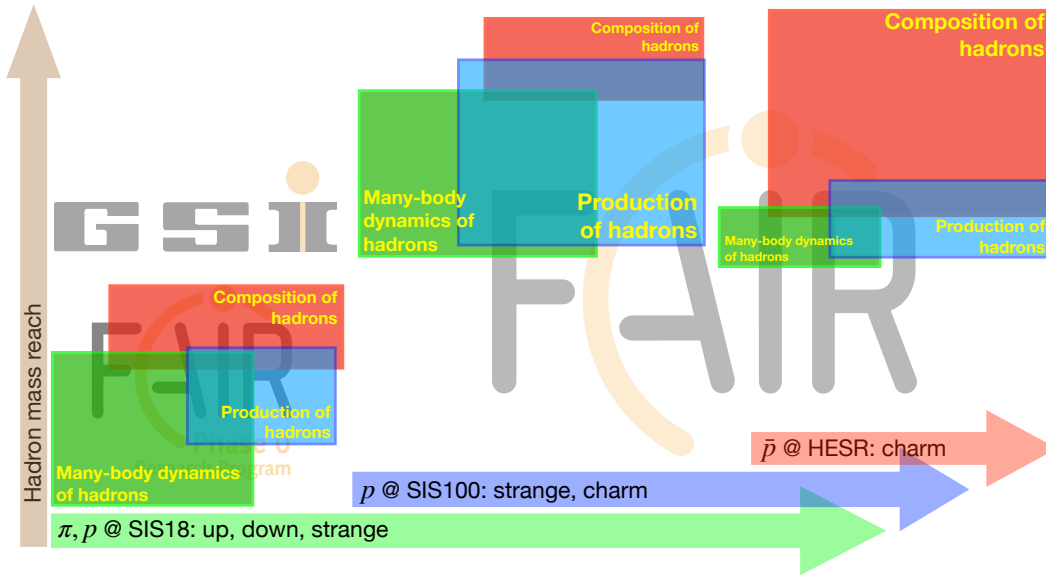


Figure 3: An illustrative sketch of the roadmap for hadron physics activities at GSI and FAIR. The initial program phase indicated by GSI/FAIR Phase-0 will exploit pion and proton beams delivered by SIS18. The two program phases marked by FAIR will exploit SIS100 providing proton and antiproton beams increasing significantly the hadron-mass reach. The three categories of boxes, distinguished by green, blue, and red, symbolize the three research domains to be tackled. The size of each box reflects its respective contribution to the overarching program.

and efficient data acquisition capabilities of the combined facility make it a powerful tool for connecting diverse physics topics across multiple fields. In this document, we outline various topics, intimately connected, that we wish to follow-up in the upcoming years.

Pion beams as part of a QCD-driven roadmap at GSI/FAIR

The physics program exploiting the pion-beam facility in combination with HADES is part of a broader hadron-physics motivated program involving the transition from GSI to FAIR. The combination of hadronic beams provided by SIS100 and versatile detector systems, such as CBM, it will be feasible to pursue a long-term and QCD-motivated program involving the three communities (nuclear, hadron, and heavy-ion physics) and driven by the experiences as obtained with the pion-beam facility and HADES. SIS100 enables to reach center-of-mass energies in the proton-proton system of about $\sqrt{s}=7.6$ GeV, thereby allowing to probe baryonic systems with single, double, and triple strangeness as well and charm-rich matter. With unprecedented beam intensities, combined with high-acceptance and versatile detector systems capable of handling high-interaction rates and utilizing free-streaming data processing, FAIR will enable precision studies in the field of QCD. On the long term, FAIR plans to realize its so-called "modularized start version" (MSVc). An essential component of MSVc is the implementation of the high-energy storage ring (HESR), specially designed to contain beams of antiprotons within an energy spectrum ranging from 0.8 GeV to 14 GeV, stochastically cooled to achieve a momentum spread of approximately $\Delta p/p \approx 10^{-5}$. Combined with a versatile, 4π detector system, PANDA, it will enable to address a wealth of complementary hadron physics topics, particularly addressing precision studies in the field hadron spectroscopy and structure [3]. Figure 3 illustrates the foreseen roadmap at GSI/FAIR.

Structure of the document

This document is organized according to the three themes that we aim to address with the pion-beam facility. In Sec. 2 we highlight some of the topics that can be explored in the field of cold matter with nuclear targets. The follow-up section 3 addresses how pion-nucleon interactions can be used to study the composition of hadronic matter. Subsequently, in Sec. 4 we describe the physics associated with the interactions among hadrons. In Sec. 5, we provide a concise description of the experimental capabilities related to the pion-beam facility and HADES. The document is supplemented with the submitted proposals to the GPAC 2025, Sec. 6, together with the various support letters, Sec. 7, received from international partners in the field, and, finally, with a member list of the HADES collaboration in Sec. 8.

2 Q : Cold matter

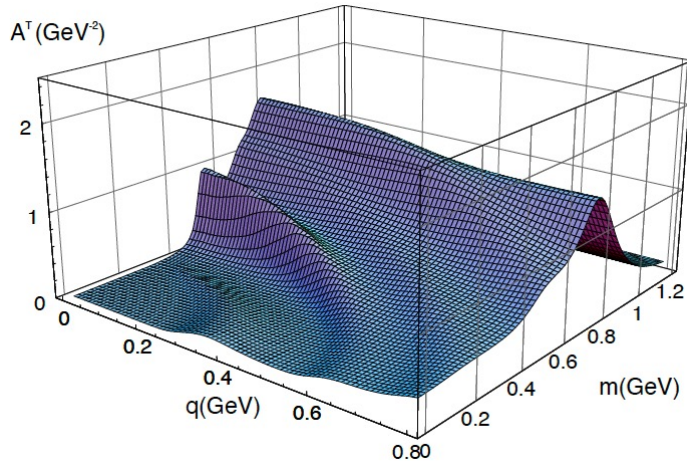


Figure 4: Transverse spectral function of the ρ meson at twice the nuclear saturation density, calculated using a hadronic model [4]. The most significant modifications are observed at small relative momenta, highlighting the medium's pronounced influence in this regime.

2.1 Introduction

A key focus of HADES, an exceptional dilepton spectrometer, is to investigate the properties and baryon couplings of vector mesons in the nuclear medium. The use of pion beams in these studies offers notable advantages, particularly due to the ideal kinematical properties of the final-state particles, such as their small relative momenta, which enhance sensitivity to medium effects. In addition to exploring the propagation of vector mesons in cold matter, it has become clear that pion beams at the highest momenta present a unique opportunity to study the production of hidden- and open-strangeness particles within the nuclear medium. Consequently, the optimal energy for these cold nuclear matter studies is $\sqrt{s} = 2.35$ GeV, which exceeds the production thresholds for ϕ -mesons and Ξ -hyperons. Overall, the total strangeness yield will increase, promoting the formation of kaons, single-strange hyperons, and hypernuclei. To achieve this energy with sufficient intensity, a high-energy primary proton beam is essential, ideally at the maximum available energy.

In addition to focusing on the high-energy part of the spectrum, there is growing interest in collecting precision data with pion beams to provide reference measurements for modeling neutrino-nucleus reactions. This has attracted significant attention from the neutrino research community. Such an experimental program can largely be carried out at lower energies, for example, at $\sqrt{s} = 1.76$ GeV using a ^{14}N primary beam, albeit at the cost of studying ϕ -mesons and Ξ -hyperons.

In the following, we briefly outline the most promising cold matter topics we identified that can be addressed at the pion-beam facility in combination with HADES. The hypernuclei aspects will be addressed in Sec. 4.

2.2 In-medium vector-meson properties

The combination of dilepton spectroscopy with a π beam offers a unique set of advantages for studying in-medium hadron properties. When compared to a p -beam, a π -beam brings in less momentum, resulting in secondary particles being produced with small recoil momentum. This recoil-less kinematics allows the particles to interact with the nuclear medium for a longer time. For penetrating probes like the decay of vector-mesons reconstructed via their dielectron decays, this setup significantly enhances the inside-to-outside fraction. The HADES experiment has a unique advantage over other experiments such as CLAS or KEK [5, 6]. It offers extensive coverage of pairs with low momenta relative to the nuclear medium, enhancing the expected modification of hadrons in nuclear matter. This is illustrated in Fig. 4, which presents the transverse spectral function of the ρ meson at twice the nuclear saturation density, calculated using a hadronic model [4]. The spectral function is shown as a function of the relative momentum with respect to the medium. The most significant modifications are observed at small relative momenta, highlighting the medium's pronounced influence in this regime. This makes HADES combined with a pion beam the ideal place to investigate line shape modification and line strength suppression due to in-medium properties of the light vector mesons ρ , ω , and ϕ as a function of momentum.

A breakthrough in cold matter studies was achieved by the measurements with HADES of the $p + Nb$ reaction at 3.5 GeV, thanks to the capability to measure dielectrons close to target rapidity, *i.e.*, at low relative momentum to the cold matter [7]. These measurements have shown a substantial modification of the in-medium ρ meson and a strong absorption of the ω . Thanks to the favorable kinematics and the specificity of pion-induced reactions to excite baryon resonances in a given range, we expect a high scientific impact from measurements in the $\pi^- + Ag$ reaction. The measurements on the carbon target will provide a reference. Some nuclear effects, such as the nucleon momentum distribution, are expected to appear in the light targets. The silver target, however, will enhance the number of decays inside the nucleus and allow investigation of effects related to changes in hadron properties in cold nuclear matter. Our primary motivation is to measure medium effects that modify the ρ and ω vector meson properties, as predicted in [8]. We estimated count rates for the e^+e^- yields from ρ and ω mesons produced in the $\pi^- + Ag$ reaction, based on a quasi-free process and scaling with $Z^{2/3}$ (see Table 1 in Sec. 3). This scaling provides an estimate of the expected yields in the absence of medium effects, which are likely to produce an excess of dielectrons below the vector meson pole due to the modified ρ contribution. A reduction of the line strength in the ω pole region in data from the Ag target, with respect to data from the C target, is also a sensitive observable for broadening of the hadron in the medium, which will be addressed. If data is taken at $\sqrt{s} = 2.35$ GeV, the ϕ meson can also be investigated within the same experimental run.

2.3 Production and propagation of strangeness

Strangeness-carrying hadrons serve as a sensitive and penetrating probe for the properties of the medium. Additionally, the kaon-nucleon and hyperon-nucleon interactions are crucial for many astrophysical processes, such as our understanding of the stability of neutron stars. The excellent particle identification (PID) capabilities and momentum resolution of HADES enable the simultaneous measurement of charged kaons, Λ hyperons, and ϕ mesons

(via their charged kaon decay channels). This facilitates a detailed study of the production and propagation of strangeness in cold nuclear matter, complementing the information gained from dilepton studies and providing relevant inputs for astrophysical questions, including neutron star stability. In particular, kaons will be used to study the kaon-nucleus potential, as demonstrated with HADES data from $p + Nb$ reactions at 3.5 GeV [7], and also investigated in the most recent $\pi^- + W$ and $\pi^- + C$ reactions at $\sqrt{s} = 2.0$ GeV [9], where strong absorption of K^- and ϕ mesons was observed. Furthermore, the formation of Λ and Ξ hyperons will be addressed. In particular, the production rate of Ξ hyperons in cold nuclear matter is crucial for understanding the observed enhancement in heavy-ion collisions. In general, such data remain scarce and, as mentioned above, are essential for constraining the Equation of State [9].

2.4 Intermediate reference for heavy-ion data

Pions are abundantly produced in heavy-ion collisions and have a high probability of interacting with the nuclear medium. Thus, pion-nucleus reactions are essential for refining theoretical models of medium effects in hot and dense nuclear matter. Pion-induced reactions offer the advantage of selectively exciting a narrow mass range of the baryon-resonance spectrum, unlike proton-nucleus reactions, which excite a broader spectrum dominated by the $\Delta(1232)$ resonance, especially at beam energies up to 3 GeV. Pion-beam interactions provide essential information about resonances with pole masses above that of the $\Delta(1232)$, data that is currently lacking for higher-lying resonances. This information will be invaluable for experiments at higher energies, such as those planned at FAIR. In summary, pion-nucleus reactions represent a critical intermediate step between elementary nucleon-nucleon or pion-nucleon collisions and the hot and dense matter created in heavy-ion (A+A) collisions. Mesons (pions, η , kaons, ...) as well as protons and light nuclei will be copiously produced, and their production spectra will serve as valuable benchmarks for hadronic models.

2.5 Input for neutrino-nucleus reaction modeling

The Long Baseline (LBL) Neutrino Oscillation Experiments are entering a new era of precision physics. In these experiments, neutrinos are produced by high-intensity accelerators (e.g., J-PARC, Fermilab), with neutrino rates increasing by a factor of approximately 20. The probability of neutrino oscillations depends on neutrino energy, mixing angles, and masses, and is precisely measured by comparing the neutrino rates, energies, and flavors at near detectors (close to the source) and far detectors (located hundreds of kilometers away).

Accurate measurement of the oscillation probability directly depends on neutrino energy reconstruction. The next generation of experiments—upgraded T2K, which began taking data this year, and the future Hyper-K and DUNE (operational by 2028/2029)—will deliver large statistics. However, reducing systematic uncertainties from the current $\sim 5 - 10\%$ to about 1-2% is crucial. The largest and most challenging uncertainties arise from modeling neutrino-nucleus interactions, primarily using hadronic models implemented in GEANT4. A longstanding issue in the LBL community is the discrepancy between models and neu-

trino cross-section measurements, especially in final states involving pion production. In T2K/Hyper-K, neutrinos in the 500-700 MeV energy range are detected via charged-current quasi-elastic interactions ($\nu_\mu + p \rightarrow \mu^- + n$) with nuclei as targets. The neutrino energy is inferred from the measured kinematics of the outgoing lepton. However, single-pion production becomes significant in the high-energy tail of the neutrino flux, particularly above 1 GeV. For DUNE, where the neutrino flux will be shifted to higher energies, pion production channels will play an even more significant role. Neutrino energy reconstruction will rely on detecting not only leptons but also pions and nucleons ($\nu_\mu + p \rightarrow \mu^- + n + N\pi$, where $N \geq 1$).

In this context, nuclear effects are critical, both at the interaction vertex and through rescattering of produced pions within the nucleus, known as Final State Interactions (FSI). Other effects like Fermi motion and Short Range Correlations must also be accurately modeled, along with secondary interactions within detector materials.

Precise hadronic models must address these factors as well as contributions from missing energy—such as undetected neutrons (relevant for T2K), re-absorbed pions, protons, or energy lost below detection thresholds (low-energy hadrons). Reliable simulations are required to correct for such systematic effects. Pion beam data are invaluable for improving model descriptions of neutrino-nucleus interactions. While the primary interaction differs between pion- and neutrino-induced reactions, the dissipation of energy within the nucleus—sensitive to nuclear properties like Fermi momentum and potential—proceeds through similar nuclear processes, including baryon resonance excitation, pion rescattering, and absorption. However, the available pion beam data is scarce and largely limited to the $\Delta(1232)$ resonance region ($p \leq 500$ MeV/c). Crucially, there is a lack of data in the energy range essential for neutrino physics, particularly for interactions like $\pi^- + \text{Fe}$, $\pi^- + \text{Pb}$ (important for T2K), and $\pi^- + \text{Ar}$ (important for DUNE), which can be filled with the current proposal.

In the previous pion beam experiment in 2014 we have studied inclusive production of p , π^+ , π^- , d , t and semi-exclusive 2- and 3-particle ($2\pi^-$, $2\pi^+$, $2p$, $\pi^+\pi^-p$...) coincident spectra with the carbon target at 0.69 GeV/c [10, 11]. This measurement provided also high statistics data at 4 other pion beam momenta of 0.61, 0.66, 0.75, 0.8 GeV/c. The aim of the analysis at 0.69 MeV/c was a benchmark of the transport models SMASH, RQMD.RMF, GiBUU and the intranuclear cascade model INCL++, used by heavy-ion and neutrino physics communities. The transport model predictions show an unexpected large dispersion, which points to the need for further adjustments. In this proposal we plan to complete the existing $\pi^- + \text{C}$ data with the measurement at 0.5 GeV/c and extend the database with the measurements at 0.5, 0.6 and 0.7 GeV/c with Fe and Pb targets. The selected energies and targets are strategic for the T2K experiment. The results will allow to test selectively the capacity of the models to describe various mechanisms like quasi-elastic, multi-pion production, rescatterings and pion absorption processes.

3 C: Hadron spectroscopy, structure, and exotics

3.1 Introduction

The results extracted from the pion-beam data on the proton target collected in 2014 around $\sqrt{s} = 1.5$ GeV, *i.e.*, within the second baryon resonance regime, highlighted the benefits and unique features of utilizing the πN interaction for baryon spectroscopy and structure studies. The N^* selectivity achieved in the πN scattering process via the s -channel offers a significant advantage over proton beams. The well-defined initial state, combined with the limited number of final-state particles, facilitates partial wave analysis, enabling the extraction of various meson couplings with excited baryons. Of particular interest are the $N^* \rightarrow \rho N$ couplings, which are highly relevant for the complementary heavy-ion program conducted with HADES. Beyond the detailed study of hadronic aspects in πN interactions, the 2014 data demonstrated the unique capability to extract valuable electromagnetic structure information by measuring the timelike form factors in the $N^* \rightarrow Ne^+e^-$ process, underlining the exceptional dilepton capabilities of HADES.

The remarkable results from the 2014 data pave the way for the planned pion-beam experiments discussed in this paper. Of particular interest is the exploration of the third resonance regime around $\sqrt{s} = 1.7$ GeV, employing the same proven methodology. Furthermore, at these higher energies, the couplings of baryon resonances excited in πN interactions to final states involving strangeness will become accessible. This will enable a systematic investigation of QCD within the framework of SU(3)-flavor symmetry. These anticipated πN studies will complement planned photoproduction experiments at CB-ELSA.

In addition to advancing studies in the baryon spectroscopy and structure sector, it will also be possible to extract valuable information on (exotic) meson-like states and glueballs through partial-wave analysis of $\pi\pi$ and $K\bar{K}$ final states produced in πN interactions at various energies. Furthermore, pion-nucleon scattering offers an ideal signal-to-background environment for investigating rare η decays.

3.2 Baryon-meson couplings

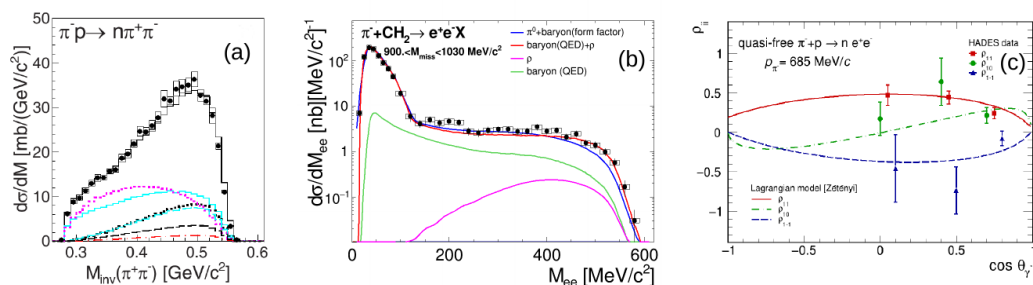


Figure 5: Panel (a) presents the $\pi^+\pi^-$ invariant mass distribution (black circles) measured with HADES in the $\pi^-p \rightarrow \pi^+\pi^-p$ reaction for a pion incident momentum of 0.685 GeV/c compared to the Bonn-Gatchina PWA solution (black solid line histogram), with the subdivision into the isobar $\Delta\pi$ (cyan), $N\sigma$ (dashed violet) and $N\rho$ (violet). The ρ contributions from s -channels (green curves) as well as from D13 (blue curve) and S11 (red curves) partial waves are also displayed. Middle and right panels present the analysis of the quasi-free $\pi^- + C_2H_4 \rightarrow n e^+e^-$ reaction at $p_\pi = 0.685$ GeV ($\sqrt{s} = 1.487$ GeV), after selection of events with $0.9 < M_{miss} < 1.03$ GeV/ c^2 . Panels (b) and (c) Distribution of e^+e^- invariant mass (M_{ee}) compared to two different phenomenological approaches: (i) baryon Dalitz decay with form factor from [12] (red) and (ii) point-like baryon Dalitz decay (green curve) + ρ (violet) (see text for details). In the first case, the contribution from π^0 Dalitz decay has also been added. Panel (c): Spin density matrix elements ρ_{11} , ρ_{10} and ρ_{1-1} extracted from the angular distributions of events with $M_{ee} > 300$ MeV/ c^2 , compared to the ones derived from the $\rho \rightarrow \pi^+\pi^-$ PWA.

channel	ε_{AR}	σ_H (mb)	σ_C (mb)	σ_{Ag} (mb)	BR	C ₂ H ₄ target		C target	Ag target
						\dot{N}_H/\dot{N}_{tot} (shift ⁻¹)	\dot{N}_C (shift ⁻¹)	\dot{N}_{Ag} (shift ⁻¹)	
$\pi^-\pi^+$ n	0.14	10	16	63	1	$3.4 \times 10^6/6.1 \times 10^6$	3.8×10^6	2.0×10^6	
$\pi^-\pi^0$ p	0.09	6.5	10.4	41	1	$1.4 \times 10^6/2.6 \times 10^6$	1.6×10^6	8.6×10^5	
$\pi^0\pi^0$ n	0.01	2	3.2	13	1	$4.9 \times 10^4/8.8 \times 10^4$	5.4×10^4	2.9×10^4	
$K^0\Lambda$	0.04	0.56	1.85	7.3	0.35	$1.9 \times 10^4/5.0 \times 10^4$	4.3×10^4	2.4×10^4	
$K^0\Sigma^0$	0.04	0.24	0.79	3.1	0.35	$8 \times 10^3/2.2 \times 10^4$	1.9×10^4	1.0×10^4	
$K^+\Sigma^-$	0.13	0.23	0.76	3.0	1	$7.2 \times 10^4/1.9 \times 10^5$	1.7×10^5	9.0×10^4	
ηn	0.01	1.2	3.96	15.6	0.39	$1.2 \times 10^4/3.1 \times 10^4$	2.6×10^4	1.4×10^4	
ωn	0.015	1.5	4.95	19.5	0.89	$4.9 \times 10^4/1.3 \times 10^5$	1.1×10^5	4.0×10^4	
$\rho \rightarrow e^+e^-$	0.25	2.1	6.93	90.3	$6 \cdot 10^{-5}$	78/204	176	95	
$\omega \rightarrow e^+e^-$	0.31	1.7	5.61	73.1	$7.4 \cdot 10^{-5}$	84/222	190	104	

Table 1: Inputs for calculation of count rates in the different channels of interest for the polyethylene (CH₂), carbon (C) and silver (Ag) targets for $\sqrt{s}=1.76$ GeV: reduction factors due to the combined acceptance and reconstruction efficiency (ε_{AR}), cross sections for π^-+p (σ_H), π^-+C (σ_C) and π^-+Ag (σ_{Ag}) reactions, branching ratios (BR). The three last columns indicate the rate of reconstructed events per shift. For the polyethylene target, the first and second numbers corresponds to interactions with protons and to the total, respectively.

Motivation

Together with photon-nucleon reactions, pion-nucleon reactions provide direct information on the electromagnetic and hadronic couplings of baryonic resonances, which are related to their intrinsic structure in terms of quarks and gluons through hadron-structure models. While the data base for photon-induced reactions has been continuously developed in the past years, the progress in the determination of the baryon spectrum and related decay properties is currently limited by the lack of precise data from pion beam experiments [13]. A better determination of the couplings of baryonic resonances to ρN and ωN final states is particularly important for the understanding of the emissivity of hot and dense nuclear matter due to the important role of intermediary vector mesons in dilepton emission. In particular baryon- ρ interactions are known to strongly contribute to the observed melting of the ρ meson in the fireball formed in heavy-ion collisions from SIS18 to LHC energies [14]. A detailed understanding of these effects requires microscopic calculations which rely on these couplings.

In a commissioning pion beam experiment in 2014, we measured the double pion production using polyethylene ((CH₂)_n) and carbon target in the second resonance region ($\sqrt{s} \simeq 1.49$ GeV [15]). The obtained two-pion ($\pi^+\pi^-$ and $\pi^-\pi^0$) data samples have been included in the multichannel Partial Wave Analysis (PWA) of Bonn-Gatchina together with other world data on single and double pion production in photon, pion and electron induced reactions, which allowed for the extraction of the various final ($\Delta\pi, \rho\pi, N\sigma$) and initial ($\frac{1}{2}^+, \frac{1}{2}^-, \frac{3}{2}^+, \dots$) resonant and non-resonant states. As the information on $\pi^+\pi^-$ and $\pi^-\pi^0$ channels from other experiments only exist as total cross sections, the HADES data were essential to constrain the ρ production (Fig. 5a) and to extract the branching ratios of the N(1440), N(1520) and N(1535) baryon resonances to the ρN channel, a basic information which is presently absent in the Review of Particle Physics. This information has then been used for the interpretation of the dielectron production [2, 16], by means of the Vector Dominance Model, as explained below. We take these results as a proof of concept of the Partial Wave Analysis method for HADES pion beam data in the two-pion production channels, which can be easily extended for other hadronic channels in the third resonance region.

At a center-of-mass energy \sqrt{s} around 1.73 GeV, many hadronic channels are open (e.g. $K^0\Lambda, \Sigma^0 K^0, \Sigma^+ K^-, \eta n, \omega n, \dots$) in addition to the two-pion production. These channels will help to constrain hadronic couplings of baryon states in this region ($\Delta(1620)$

$1/2^-$, $\Delta(1700) 3/2^-$, $N(1650) 1/2^-$, $N(1675) 5/2^-$, $N(1680) 5/2^+$, $N(1710) 1/2^+$, $N(1720) 3/2^+$, \dots) which are very poorly known. Our goal will therefore be to provide statistically-unprecedented differential data for hadronic channels, including those with neutral mesons. Together with complementary photoproduction data taken in a similar center-of-mass energy at CBELSA combined with our close collaboration with corresponding colleagues both from experiment and theory, *e.g.* Bonn-Gatchina group, we expect to make a strong impact in our understanding of the light baryon spectrum in this energy interval. The two-pion channels with a cross section of the order of 6.5-10 mb can be measured with a very large statistics and will provide new determinations to the $2\pi N$ channels, and especially to ρN which has a strong impact for medium effects, as mentioned above. Resonant final states of the type $N(1440)\pi$, $N(1520)\pi$, \dots also attract much interest since they are related to the three body nature of baryonic resonances, which might be a dominant decay mode in the case of the unobserved (or "missing") resonances. The study of 2π production in photo and electro-production was also recently used to provide evidence for a new $N'(1720) 3/2^+$ resonance [17], with a mass lower by 20 MeV and very different ρ and electromagnetic couplings with respect to the known $N(1720) 3/2^+$ resonance. By providing complementary data from pion induced reactions, our experiment can bring a timely contribution to this hadron structure highlight. The data base for the ηn , $K\Lambda$ and $K\Sigma$ channels also need to be improved, which can in particular be used to firmly establish the existence of other resonances.

Expected results

Although good precision differential spectra are badly missing, the total cross sections for hadronic channels in $\pi^- + p$ reactions in the region between 1.68 and 1.8 GeV are in general known with a precision of 10-20% and the reconstruction efficiencies of exclusive channels can be estimated based on previous analyses of HADES data, as [15] for the charged double pion production (see Table 1).

The reconstruction of the neutral hyperon production can be most efficiently achieved using the K_S^0 production corresponding to half of the cross section in the corresponding exclusive K^0 production channel. The reconstruction of K_S^0 via their decay into $\pi^+\pi^-$ decay is used, with a branching ratio of 69% and an efficiency of $\varepsilon_{AR} = 4\%$, as deduced from full scale GEANT simulations, which were validated by previous reconstructions of K_S^0 in HADES experiments. The missing mass resolution of $\sigma = 11 \text{ MeV}/c^2$, as measured in previous experiments is then sufficient to resolve the Λ and Σ^0 states. For the $\Sigma^- K^+$, an efficiency of 13% is estimated. For the η and ω production, we use the decay into $\pi^+\pi^-\pi^0$, which can be reconstructed with efficiencies of 1 % and 1.5% for η and ω , respectively, as deduced using simulations including the ECAL.

The count rates for the carbon target need also to be estimated, as they contribute to the statistical errors for the measurement of the $\pi^- + p$ reaction obtained by subtraction of pion-carbon interactions from the polyethylene data. Hadronic channels in π -A reactions are also interesting by themselves, for cold matter studies, as developed further below. We therefore give count rates for measurements on the carbon and silver targets for the above-mentioned channels. Inclusive meson production will be measured with even higher yields. Reaction cross-sections measured for pion-nuclei reactions scale as $A^{2/3}$ [18]. However, for the production of pions, which undergo strong absorption already in carbon, we used a ratio $\sigma_C/\sigma_p = 1.6$ as measured at $\sqrt{s}=1.49 \text{ GeV}$. For the exclusive strangeness production channels, we neglect the absorption and deduce the cross sections for the reaction on carbon and using the relation $\sigma \sim Z^{2/3}$, as mainly protons are involved.

3.3 Electromagnetic couplings

Motivation

Virtual photons originating from baryonic matter provide a means to probe the electromagnetic currents and structures underlying various processes. The use of these probes offers several advantages, stemming from the fundamental principles of quantum electrodynamics (QED). From a heavy-ion perspective, virtual photons are not affected by final-state interactions, enabling direct exploration of the medium. From the standpoint of hadron physics, the couplings of virtual photons, governed by QED, facilitate systematic analyses of the electromagnetic structure of hadronic matter and their transitions, offering an unambiguous sensitivity to the fundamental structure of hadrons. HADES brings extensive expertise in utilizing virtual photons, primarily through dilepton detection, to study baryonic matter in heavy-ion collisions as well as in elementary processes.

HADES experiments performed in the last years in proton-nucleus [7] or nucleus-nucleus [14] reactions have demonstrated an excess radiation of e^+e^- above conventional sources, for invariant masses below the vector meson poles, attributed to emission out of the hot and dense stage of the reaction (fireball). The most successful explanation is that this radiation emerges from decays of far off-shell ρ mesons with a strongly modified spectral function due to their coupling to baryonic resonances in hadronic matter. The study of elementary reactions, like $p+p$, quasi-free $n+p$ and π^-+p [2, 16, 19–21], emphasized further the importance of intermediary ρ mesons in baryon resonance Dalitz decays ($N/\Delta \rightarrow Ne^+e^-$, in accordance with the Vector Dominance Model (VMD) (see Fig. 1, Right (b)). Pion beam experiments provide an increased sensitivity to these effects, as the resonances are excited in the s -channel in a narrow mass bin, corresponding to the pion beam momentum dispersion. This limits the overlap between many baryon states, which is unavoidable in the case of nucleon-nucleon reactions. In addition, the study of the exclusive channel $\pi^-+p \rightarrow ne^+e^-$ can be achieved by the simple detection of the e^+e^- pair with a neutron missing-mass cut. Therefore, the $\pi^-+p \rightarrow ne^+e^-$ reaction is an ideal tool to study the electromagnetic structure of baryon transitions in the region of small positive four-momentum transfer squared ($q^2 = M_{ee}^2$), where vector meson poles play an important role. This information is complementary to the one obtained in electron scattering experiments in the space like region ($q^2 < 0$) and is therefore needed for a global understanding of these transitions.

Lessons from the 2014 data

The differential cross sections in the $\pi^-+p \rightarrow ne^+e^-$ reaction can be parameterized in a model independent way using different equivalent functions (helicity amplitudes, form factors or density matrix elements), which contain information on the electromagnetic structure of the baryon transitions. In particular, in the context of the HADES program, the interest of studying the $\pi^-+p \rightarrow ne^+e^-$ reaction is to check the validity of the Vector Dominance model (see Fig. 1) for baryon electromagnetic transitions, which is used for the interpretation of the e^+e^- production in terms of modified ρ meson spectral function. The commissioning experiment performed in 2014 using polyethylene and carbon target confirmed the relevance of the $\pi^-+p \rightarrow ne^+e^-$ channel to investigate time-like electromagnetic transitions and in particular test VMD. In the previous experiment in 2014, we measured

the e^+e^- production from polyethylene and carbon targets at a πN center-of-mass energy of $\sqrt{s}=1.49$ GeV, close to the pole of the N(1520) resonance. The statistics for e^+e^- events recorded on the carbon target was not sufficient to make an accurate subtraction and isolate π^-+p interactions, however, the quasi-free character of the e^+e^- production in the π^-+C reaction could be carefully checked and was taken into account in the modeling of the π^-+PE reaction using a quasi-free participant-spectator model. The expected M_{ee} invariant mass distributions for the $\pi^-+p \rightarrow n e^+e^-$ channel can be estimated from the known $\gamma n \leftrightarrow \pi^-+p$ cross-sections in a simple QED calculation, assuming a point-like vertex (dashed green line in Fig. 5b). To estimate the effect of time-like electromagnetic form factors, which are expected to modify the yield at large M_{ee} , we used models recently developed for the N-N(1520) [12] and N-N(1535) [22] transitions, where baryons are described with a quark core and a meson cloud, with parameters fitted to existing data in the space-like region. They cause a significant enhancement of the dielectron yield at large M_{ee} w.r.t the QED calculations and provide a quantitative description of HADES data.

We also adopted an alternative approach using the ρ meson mass distribution obtained in the PWA of the $\pi^-+p \rightarrow \pi^+\pi^- n$ reaction, as explained above. The corresponding e^+e^- invariant mass distribution was calculated using VMD, which yields a dependence of the $\rho \rightarrow e^+e^-$ meson branching ratio $BR(M) \sim M_{ee}^3$ and this contribution was added to the point-like e^+e^- emission. This "two-component" approach provides a modeling of the time-like electromagnetic baryon transition form factor in terms of two components: a photon and a ρ meson coupling. It is noticeable that both approaches give quantitatively the same results, in good agreement with the data.

Extracting spin-density matrix elements

HADES results also demonstrate that isoscalar (ω) contributions play a minor role in e^+e^- production in the second resonance region, in contrast to the earlier predictions [23].

Further information, in particular on the transverse and longitudinal virtual photon polarization can be obtained from the angular distributions. A convenient parameterization of the amplitudes $|A|$ at a given value of M_{ee} and emission angle of the virtual photon derives from the density matrix formalism [24].

$$|A|^2 \propto 4k^2[2\rho_{00}(1 - \cos^2\theta) + 2\rho_{11}(1 + \cos^2\theta) + 2\sqrt{2}\sin(2\theta)\cos\phi Re\rho_{10} + 2\sin^2\theta Re\rho_{1-1}\cos(2\phi)]. \quad (1)$$

Here, k^2 , θ and ϕ denote the momentum, polar angle and azimuthal angles of the lepton in the virtual photon reference frame, respectively, and ρ_{00} , ρ_{11} , ρ_{1-1} are the three independent density matrix coefficients which can be expressed, for a transition of given spin and parity, as a function of helicity amplitudes or transition form factors. A method to extract spin density matrix elements from a fit to experimental data has been developed taking into account acceptance and efficiency effects [2]. Despite the low statistics which affected the precision of the data in the 2014 experiment, and the low acceptance for backward virtual photon angles in the center-of-mass, the coefficients were studied in three bins of center-of-mass angle of the virtual photon for $M_{e^+e^-} > 0.14$ GeV/ c^2 , as shown in Fig. 5c. The deviations of ρ_{11} from 0.5 and ρ_{10} from 0 clearly demonstrates the contributions of virtual photons with longitudinal polarization, in contrast to real photons. Besides, non-zero $\rho_{-1,1}$ values signal important contributions of transitions with spin larger than $\frac{1}{2}$, which is consistent with the dominance of the N(1520) resonance found in the two pion analysis [15]. Indeed, the values of the spin density matrix elements are found in good agreement with

the predictions of the model of [24] for the N-N(1520) transition, calculated with a VMD form factor.

The density matrix formalism was also applied to analyze the angular distributions of pions from the $\rho \rightarrow \pi^+\pi^-$ component in the PWA solution, and a good consistency was obtained with the coefficients obtained from the dilepton distributions (curves on Fig. 5). This is an additional very direct test of the VMD approach, in complement to the successful description of the invariant mass spectra.

Towards the third resonance regime

The results from the 2014 data provide the very first and promising information about the baryon electromagnetic transitions in the time-like region and motivate the exploration of the third resonance region, using the same approach. To demonstrate the feasibility of the measurement at higher energy, we developed full scale simulations of the $\pi^- p \rightarrow X e^+ e^-$ reaction. For the Dalitz decays of π^0 and η mesons ($\pi^0, \eta \rightarrow \gamma e^+ e^-$), which constitute the dominant contributions, the production cross sections from previous experiments were used [25,26]. e^+e^- emission from intermediate $\Delta(1232)$ Dalitz decay ($\Delta(1232) \rightarrow N e^+ e^-$) is also taken into account, using $\Delta\pi$ cross sections from a Bonn-Gatchina PWA solution of the $\pi^- p$ reaction, but has a much smaller contribution. For the simulation of the $\pi^- p \rightarrow n e^+ e^-$ exclusive channels considered here as our signal, we used the two-component approach, which was successful for the data in the second resonance region, as described above. Following the analysis of the $\pi^- p \rightarrow n \gamma$ reaction around $\sqrt{s} = 1.76$ GeV, the N(1675) and $\Delta(1700)$ baryon resonances were identified as providing the most important contributions, due to their large γN couplings. The ρ production cross sections is taken from the HSD model [27] (2.1 mb at $\sqrt{s} = 1.76$ GeV), which accounts for the coupling of the ρ meson to baryon resonances. The higher (30 %) branching ratio for the ρ decay

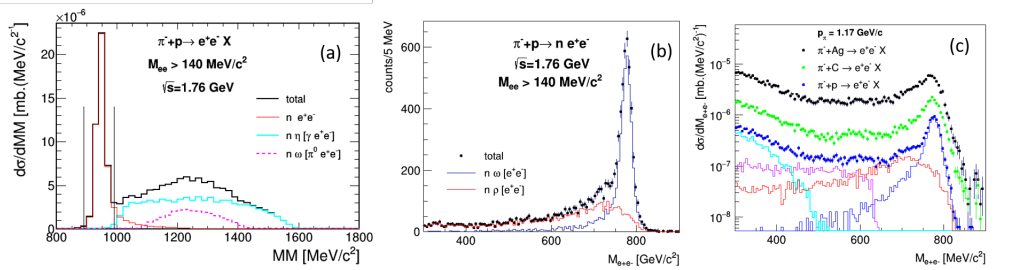


Figure 6: Simulations of the reaction $\pi^- p \rightarrow X e^+ e^-$ at $p_\pi = 1.16$ GeV/c including all known sources of dileptons. (a) Missing mass (M_{miss}) distribution for events with invariant mass $M_{ee} > 140$ MeV/c². (b) Expected distribution of counts in 5 MeV bins as a function of the invariant mass after selection of the exclusive channel using the condition on the missing mass $0.9 < M_{\text{miss}} < 1.03$ GeV/c². (c) Expected reconstructed inclusive e^+e^- invariant mass spectra for measurements on the silver target (black dots), carbon target (green dots) and for interaction with protons in the polyethylene targets (blue dots). The cyan, violet, red and blue curves display the $\eta \rightarrow e^+e^-$, $\omega \rightarrow \pi^0 e^+e^-$, $\rho \rightarrow e^+e^-$ and $\omega \rightarrow e^+e^-$ contributions.

into e^+e^- of $6 \cdot 10^{-5}$ w.r.t. the one at pole is due to the enhanced production of low mass ρ mesons due to the coupling to baryons. Note, that these values strongly depend on the coupling of baryon resonances to the ρN channel, which will be extracted from the PWA analysis of the $\pi^+\pi^- n$ and $\pi^0\pi^- p$.

As the ω spectral function is expected to be less sensitive to the coupling to baryons, we took measured cross sections for the $\pi^- p \rightarrow \omega n$ reaction, known with a precision of about 10% from measurements at Rutherford Laboratory using neutron detection and missing mass [28]. For the combined acceptance and reconstruction efficiency of e^+e^-

pairs produced from ρ and ω , we find values of 25% and 31% respectively from GEANT simulations, taking into account in particular the improved efficiency of the e^+e^- pair reconstruction provided by the upgraded RICH detector.

The choice of a center-of-mass energy 40 MeV above the ω production threshold allows for a detailed study of the ω meson spectral function, which will serve as a reference for studies of omega absorption in nuclei, as discussed in the next subsection.

In the region below the ω peak, significant interferences between the isoscalar (" ρ -like") and the isovector (" ω -like") e^+e^- productions might be present, as predicted by [23, 29] and could be studied as well. We also plan to analyze the electron angular distributions and extract the spin density coefficients ρ_{11} , ρ_{10} and ρ_{1-1} to get more specific information on the nature of the transitions as a function of the M_{ee} invariant mass. We will therefore measure the spin density matrix elements in the three bins of invariant masses ([300-600], [600-700] and [700-900] MeV/ c^2) and the three bins of the virtual photon angle ([-0.02,0.03], [0.3,0.6] and [0.6,0.95]). According to the results of the previous experiment and detailed simulation studies, such a binning in angle is well suited to characterize transitions from baryonic resonances with spin larger than 1/2. However, we would like to improve the precision of each fit by increasing the statistics by at least a factor 10, i.e. we aim at 5000 e^+e^- events in each mass bin.

Although models for electromagnetic baryon transitions in the third resonance region are scarce, the new data offers an opportunity to extend approaches like those proposed in [12, 24] for the second resonance region. Previous investigations into the electromagnetic structure of baryon transitions have sparked significant theoretical interest in computing electromagnetic transition form factors. A range of models exists, utilizing non-perturbative techniques [30, 31], as well as model-independent frameworks with methodologies allowing systematic improvements [32, 33]. These advancements provide a robust foundation for high-statistical-precision data to be compared with cutting-edge theoretical approaches, yielding definitive insights.

3.4 Exotic mesons

The spectrum of scalar mesons remains one of the most intriguing and yet under-explored areas in hadron spectroscopy. This field has gained particular significance with the growing interest in exotic mesons. Within this sector, one expects to find the lowest glueballs, four-quark systems, hybrid states, and bound states of other mesons. Notably, many of these states manifest as scalar mesons, including:

- $f_0(500)$ (σ), often interpreted as a mix of two-quark and four-quark components with a small glueball admixture;
- $f_0(980)$ and its isospin-1 counterpart $a_0(980)$, viewed as two-quark bound states of $K\bar{K}$;
- $f_0(1370)$, typically identified as a two-quark state;
- $f_0(1500)$, suggested to be a mixture of two-quark and glueball contributions;
- $f_0(1710)$, which is likely the lowest pure glueball state.

These interpretations remain largely speculative, albeit grounded in decades of theoretical research spanning over 30 years. Unfortunately, the lack of new and precise experimental data has left many of these hypotheses unresolved.

The last comprehensive experimental investigations of scalar amplitudes date back to the late 1970s and early 1980s, carried out by the CERN-Krakow-Munich collaboration. These studies provided an extensive database and partial wave analyses of two-pion effective masses up to approximately 1800 MeV (see Fig. 7). For their time, these results were groundbreaking but were also subject to significant uncertainties, such as the "up-down" ambiguity below 1000 MeV and multiple conflicting solutions.

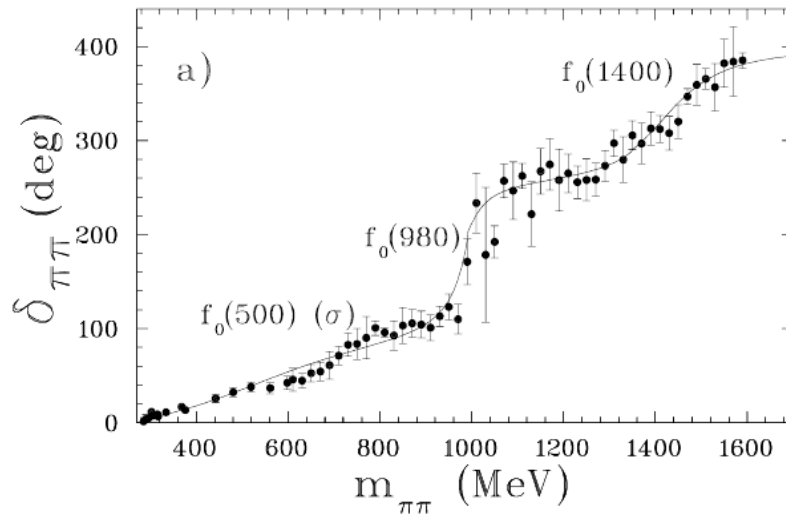


Figure 7: The $I=0$, S-wave phase shift for the $\pi\pi$ interaction obtained from the fit to the experimental data. The theoretical framework is based on dispersion relations with imposed crossing symmetry condition for the $\pi\pi$ interactions [34–36].

All uncertainties and ambiguities were systematically addressed through theoretical developments. These efforts were grounded in Roy's dispersion equations from the 1970s and extended by the GKPY dispersion equations introduced around 2010 [34–36]. The new equations significantly reduced the average error in amplitude calculations, shrinking the allowable range of possible amplitudes by a factor of about six. The work of the Madrid-Krakow group on GKPY equations, alongside efforts by the Bern group on Roy equations, culminated in major updates to the scalar meson sector of the Particle Data Tables in 2012. Notably, the meson $f_0(500)$ received a new designation, along with substantially revised mass and decay width parameters. Despite substantial theoretical advances in the analysis of amplitudes from the $\pi\pi$ threshold up to approximately 1800 MeV, the region around 1000 MeV remains particularly enigmatic. This range is dominated by the narrow $f_0(980)$ state, which induces rapid amplitude variations. Analyzing these changes demands highly accurate, densely sampled experimental data (see Fig. 7). The internal structure of $f_0(980)$ and its partner $a_0(980)$ has been the subject of numerous theoretical studies, but none has provided a definitive characterization. Precise experimental data in the $\pi\pi$ and $K\bar{K}$ channels around the 1000 MeV region could significantly advance our understanding of meson spectroscopy and offer the first conclusive evidence for hypothesized mixed structures. Using a pion beam at momenta around 2.3 GeV/c, HADES can deliver precise data in key channels essential for theoretical coupled-channel studies. These include the $\pi\pi$ and $K\bar{K}$ channels in the S0 wave, $\eta\pi$ and $K\bar{K}$ in the S1 wave, and $\omega\pi$ in the P1 wave.

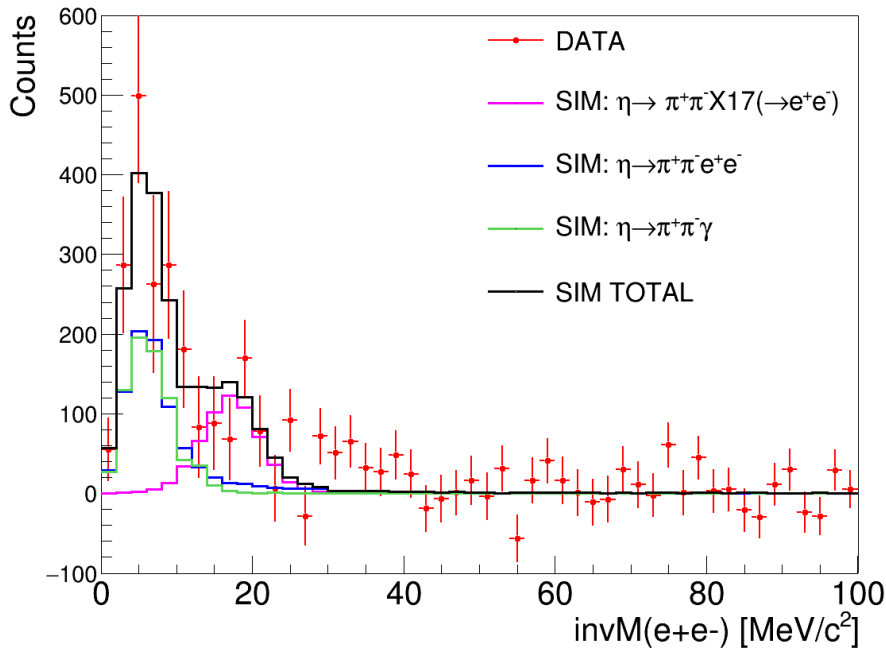


Figure 8: Preliminary invariant mass of e^+e^- pairs obtained for inclusive η production in proton-proton collisions at 4.5 GeV, decaying into $\pi^+\pi^-e^+e^-$. The data are compared to simulations which represent main background sources and the $X(17)$ signal.

3.5 Rare eta meson decays

One of the key challenges in modern experimental physics is to test the validity of Standard Model (SM) predictions and search for hints of new phenomena that fall outside its established framework. While the Standard Model provides an excellent description of particles and their interactions, it fails to explain certain fundamental issues, such as the matter-antimatter asymmetry in the Universe and the origin of neutrino masses.

An important area of both theoretical and experimental investigation is the CP problem inherent in the Standard Model. CP-violating processes have been observed in weak decays, such as K_L leptonic decays (studied by the KTeV [37] and NA48 [38] collaborations) and in B meson decays (investigated by Belle [39] and BaBar [40–43]). However, the CP violation observed so far in the electroweak sector, originating from quark mixing described by the CKM matrix, is far too small to account for the observed matter-antimatter asymmetry.

Moreover, a possible violation of CP in the strong interaction would lead to a finite neutron electric dipole moment, which experimentally is considered to be very small, less than 10^{-10} [44, 45]. The absence of CP violation in the strong interaction could potentially be explained by the existence of hypothetical light-mass QCD Axions, which are not included in the Standard Model. This was postulated by Weinberg and Wilczek which was part of the electroweak Higgs sector and a common breaking mechanism for the electroweak and Peccei-Quinn symmetries with a predicted mass range of $\mathcal{O}(100 \text{ keV} - 1 \text{ MeV})$.

Recent theoretical work [46–48] has extended this hypothesis, suggesting that QCD axions with masses in the MeV range could exist. These axions are assumed to couple predominantly to the first-generation Standard Model quarks, be short-lived, decay primarily into e^+e^- pairs, and have suppressed isovector coupling to cancel leading-order χ PT contributions to axion-pion mixing. Under this framework, hadronic decays of η and η' mesons

become valuable probes for QCD axions and axion-like particles. The most promising channels are three-body final states such as $\eta^{(\prime)} \rightarrow \pi^0\pi^0 a(e^+e^-)$ and $\eta^{(\prime)} \rightarrow \pi^+\pi^- a(e^+e^-)$, where a denotes the axion-like particle. Additionally, the observation of a "bump-like" excess (the so-called Atomki Anomaly) in the invariant mass distribution of e^+e^- pairs emitted during the de-excitation of specific states of ^8Be and ^4He nuclei [49, 50] has been interpreted as evidence of a piophobic QCD axion with a mass of 17 MeV, referred to as the $X(17)$ particle.

The HADES detector with its capability for detecting low-mass e^+e^- pairs can be used for studies of the rare η decays and particularly to search for the $X(17)$ particle. In this context, assuming a dominant decay of the potential QCD axion into a dilepton pair e^+e^- , one can benefit from the very high reconstruction efficiency and access to low-mass regions with low momentum in the HADES detector. Sensitivity to the coupling of the axial-vector axion to the e^+e^- has been proven using the p+p data collected with HADES at 4.5 GeV, see Fig. 8.

The η signal has been reconstructed using the decay $\eta \rightarrow \pi^+\pi^- e^+e^-$ and the preliminary upper limit of the branching ratio $\text{BR}(\eta \rightarrow \pi^+\pi^- X17)$ has been estimated to be $< 2.58 \times 10^{-5}$, however the multi-pion background contribution is very large resulting in a low signal to background ratio. The experiment with the pion beam offers a unique possibility to study the η decay in a practically background-free exclusive reaction $\pi^- + p \rightarrow n + \eta$, with a neutron tagging using the missing mass method.

4 *D: Effective interactions*

4.1 Introduction

This section of the paper focuses on pion-beam studies aimed at extracting valuable insights into baryon-meson interactions at low energies within the SU(3)-flavor framework. In particular, this includes experiments investigating hyperon-nucleon and hyperon-meson interactions.

For the hyperon-nucleon interaction, the studies aim to determine hyperon polarization in πN interactions. This information is essential for follow-up investigations into the spin degrees of freedom in hyperon-nucleon interactions, utilizing secondary polarized hyperon "beams" in planned experiments at J-PARC. Additionally, it provides critical observables for partial-wave analyses in baryon spectroscopy studies, as outlined in Sec. 3. Furthermore, pion beams interacting with nuclear targets offer an excellent source for hypernuclei production, whose properties provide deeper insights into the low-energy aspects of the hyperon-nucleon interaction.

In addition to studies on the hyperon-nucleon interaction, we also plan to investigate the hyperon-meson interaction through final-state interaction studies. These measurements complement CP-violation studies in the hyperon sector conducted by BESIII and HyperCP, particularly by providing precise determinations of the strong-phase difference via $\pi\Lambda$ final-state interactions.

4.2 Hyperon polarization

In the 1970s a large transverse polarization of Λ hyperons has been discovered in unpolarized proton-beryllium collisions. Since then, similar polarization has been observed in various collision systems, lepton-hadron deep-inelastic, hadron-hadron, hadron-nucleus and electron-positron collisions. There exists many theoretical approaches, some of them are successful [51, 52], however none of them is able to describe the world data in a consistent way. The nonzero recoil polarization is also observed for other hyperons Σ or Ξ . Studies of this phenomenon is crucial not only for understanding of the strangeness production mechanism but also to obtain the fundamental information about the hyperon-nucleon (Y-N) interaction and nuclear forces by performing secondary two-body Y-N scattering experiments. Studies of polarization observables like analyzing powers or depolarization can give new insight in the nuclear forces and dynamics in such systems. The former hyperon (Λ , Σ^0) polarization data measured in the pion beam experiments [53–55] suffer from large statistical errors and also uncontrolled systematic errors. Precise polarization determination and identification of angular regions with the highest polarization can be very useful for designing future measurements with secondary hyperon beams, like the J-PARC experiment [56, 57]. J-PARC will use high intensity $\pi^{+/-}$ beams to perform precise N^* baryons spectroscopy and measurements of spin observables of the Λ -p scattering with a polarized Λ secondary beam [57]. Since HADES is a versatile experiment it can help to identify physics problems to be studied with the high precision upcoming experiments. Precise polarization determination along with differential cross sections are also important for the partial wave analysis [58] and for coupled-channel models [55] to identify various resonance contributions. A measurement of the Σ^0 recoil polarization in $\pi^- p \rightarrow K^0 \Sigma^0$ is crucial for the determination of the $D_{33}(1700)$ and $P_{33}(1920)$ resonances.

The measurement with the pion beam opens a possibility to study the Λ and Σ^0 self-polarization. The Λ polarization is expected to be very large $\sim 100\%$ in this energy range [53], while for Σ^0 [54] only few data points exist with very large statistical errors. To

measure the Lambda polarization K^0 reconstruction via 2 pion decay ($\pi^+\pi^-$) is assumed and the third particle, either pion or proton, is needed to extract the polarization value P_Λ using its angular distribution ($\cos(\beta)$) in the Λ reference frame. The angular distribution of the decayed pion or proton in the rest system of Λ with respect to some reference axis is given by the formula:

$$\frac{1}{N_0} \frac{dN}{d\cos(\beta)} = 1 + \alpha P_\Lambda \cos(\beta), \quad (2)$$

where N_0 is the "unpolarized" yield of the decay hadron, α is the decay asymmetry parameter, which was recently updated as $0.750 \pm 0.009 \pm 0.004$ [59], $P_\Lambda = P_\Lambda(\cos\theta_\Lambda^{CM})$ is the Λ polarization and θ_Λ is the Λ scattering angle.

To estimate the expected count rates the full scale simulations of the $\pi^-p \rightarrow \Lambda K^0$ and

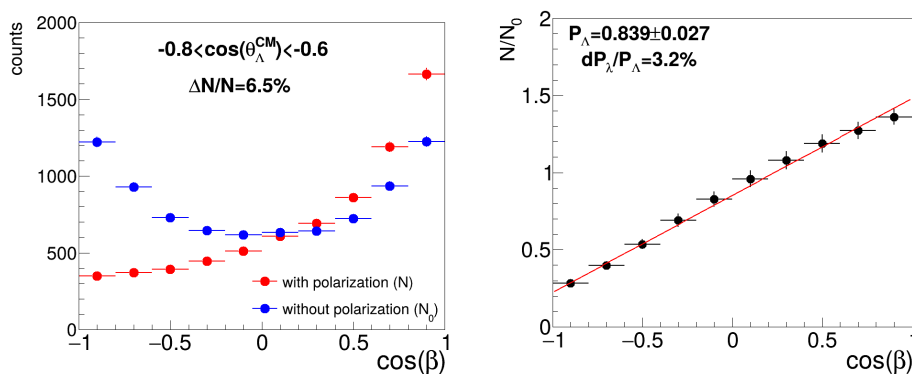


Figure 9: Left panel: expected statistics in the distribution of the emission angle of the decayed proton with (N - red points) and without polarization (N_0 - blue points) in a given range of $\cos\theta_\Lambda^{CM}$ for $\pi^-p \rightarrow \Lambda K^0$ at $\sqrt{s} = 1.73$ GeV for 7 shifts on the CH_2 target. The estimated statistical accuracy is $\sim 6.5\%$. Right panel: same as in the left panel but for the ratio of the "polarized" (N) and "unpolarized" (N_0) distributions. The estimated statistical accuracy of the extracted from the linear fit polarization is $\sim 3\%$.

$\pi^-p \rightarrow \Sigma^0 K^0$ reactions has been performed including the realistic angular distributions of Λ [53, 55] and Σ^0 [54]. Fig. 4.2, left panel presents a sample distribution of the expected "unpolarized" N_0 and "polarized" N (N_0 distribution weighted according to the Eq. 2) count rates in a function of the $\cos(\beta)$ in a selected bin of $\cos(\theta_\Lambda^{CM})$. The polarization value has been obtained from a linear fit to the N/N_0 ratio distribution, as visible in Fig. 4.2, right panel. We aim at precise determination of the Λ polarization at 5 energy points: $\sqrt{s} = 1.67$ GeV, $\sqrt{s} = 1.70$ GeV, $\sqrt{s} = 1.73$ GeV, $\sqrt{s} = 1.73$ GeV and $\sqrt{s} = 1.79$ GeV.

Σ^0 polarization will be measured in the longest run at $\sqrt{s} = 1.76$ GeV with expected statistical accuracy of 7%. Since Σ^0 decays electromagnetically into $\Lambda + \gamma$, the Λ decay into $p\pi^-$ will be used as an analyzer of the Σ^0 self-polarization.

So far the Λ and Σ^0 polarization has been measured with very low accuracy of $\sim 20\%$ [53, 54]. In this experiment we aim to measure the polarization with the unprecedented precision of $\sim 6\%$.

4.3 Hypernuclei formation

Hypernuclei offer an additional way to investigate the hyperon-nucleon ($Y-N$) interaction. The small recoil momentum of secondary particles produced in meson beams is particularly advantageous for the formation of hypernuclei [60]. Our research has demonstrated that

the particle identification (PID) and vertex reconstruction capabilities of HADES, combined with the use of an artificial neural network (ANN), are well-suited for reconstructing hypernuclei and performing precise measurements of their lifetimes and branching ratios [61]. These capabilities allow the extraction of relevant information about the Y - N interaction from hypernuclei data within the same experimental run.

Fig. 10 shows the invariant mass distribution of π^- and ${}^3\text{He}$ pairs from the $\pi^- + W$ data taken in 2014. A signal of the hypertriton with about 120 counts and a significance of 5.3 emerges above the mixed-event background.

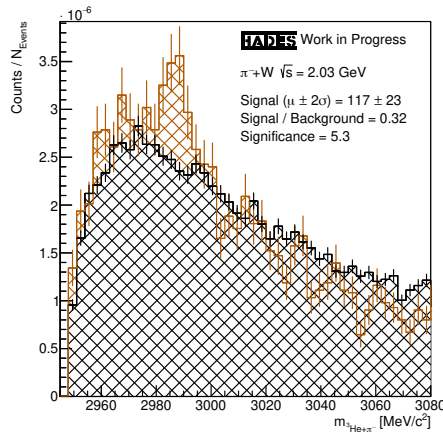


Figure 10: Invariant mass distribution of π^- and ${}^3\text{He}$ pairs from the $\pi^- + W$ data taken in 2014 (orange). A signal of the hypertriton with about 120 counts and a significance of 5.3 emerges above the mixed-event background (black).

matter aim to leverage significant improvements in the pion beam properties and detector technologies compared to the 2014 experiment. Hence, the anticipated future beam time will offer substantial enhancements over the 2014 experiment leading to an overall gain factor of 100. This significant increase in efficiency and data collection capability translates into an expected production of approximately: 10000 hypernuclei. These yields represent an up to now unmatched amount, (almost an order of magnitude increase) of hypernuclei statistics at GSI and will enable statistically robust studies of hypernuclei properties, including lifetimes, branching ratios, and formation dynamics.

4.4 Hyperon-meson interaction

The Standard Model (SM) successfully describes fundamental particles in particle physics but does not provide a satisfactory explanation for the matter-antimatter asymmetry in the Universe. This phenomenon can be explained by the existence of processes that violate the combined charge conjugation and parity (CP) symmetry [62]. The existence of CP violation consistent with the SM expectation was confirmed in kaon, beauty and charm mesons decays and in the bottom baryon sector. A very sensitive test of CP violation and effects beyond SM is offered by the hyperons (Y) decays [63]. Hyperons weak decays involve two amplitudes: a parity conserving P-wave (parity-even), and a parity violating S-wave (parity-odd). CP violation can be observed if there is interference between CP-even and CP-odd terms in the decay amplitude. A CP violation signal in the hyperon decays has been recently extracted in the BESIII and HyperCP [64] experiments. The BESIII collaboration has developed a new and very sensitive method to study the CP

violation effects using sequentially decaying entangled baryon-antibaryon pairs produced in the $e^+e^- \rightarrow J/\psi \rightarrow \Lambda\bar{\Lambda}/\Xi^-\bar{\Xi}^+$ processes [65]. They have extracted the numerous Ξ^- and Λ decay asymmetry parameters, also for its charge-conjugate channel [59, 66, 67]. In this framework the leading-order contribution to the CP asymmetry A_{CP}^Y is given as: $A_{CP}^Y \approx -\tan(\delta_P - \delta_S)\tan(\xi_P - \xi_S)$, where $\delta_P - \delta_S$ denotes the strong-phase difference of the final-state interaction (FSI) between the Λ and π^- from the Ξ^- decay, and $\xi_P - \xi_S$ denotes the weak-phase difference. CP-violating effects would manifest themselves in a nonzero weak phase. The weak-phase difference has been directly determined for the decay $\Xi^- \rightarrow \Lambda\pi^-$ using entangled Ξ^- and $\bar{\Xi}^+$ [66]. The strong-phase difference has been determined indirectly using the two other decay parameters $\langle\phi^\Xi\rangle$ and $\langle\alpha^\Xi\rangle$. This is one of the most precise tests of the CP symmetry for strange baryons.

To gain direct and more precise information on the strong-phase difference and increase the sensitivity to CP violation effects, the knowledge on the $\Lambda - \pi^-$ FSI, which enters the calculations, is needed. Such effect can be studied with the HADES detector and pion beams in the three-body $\pi^- + p \rightarrow \Lambda + \pi^- + K^+$ reaction. Using a partial wave or Dalitz plot analysis the $\Lambda - \pi^-$ FSI effects can be pin-down. These studies will be complementary to measurements planned at the JLab facility with photon beams.

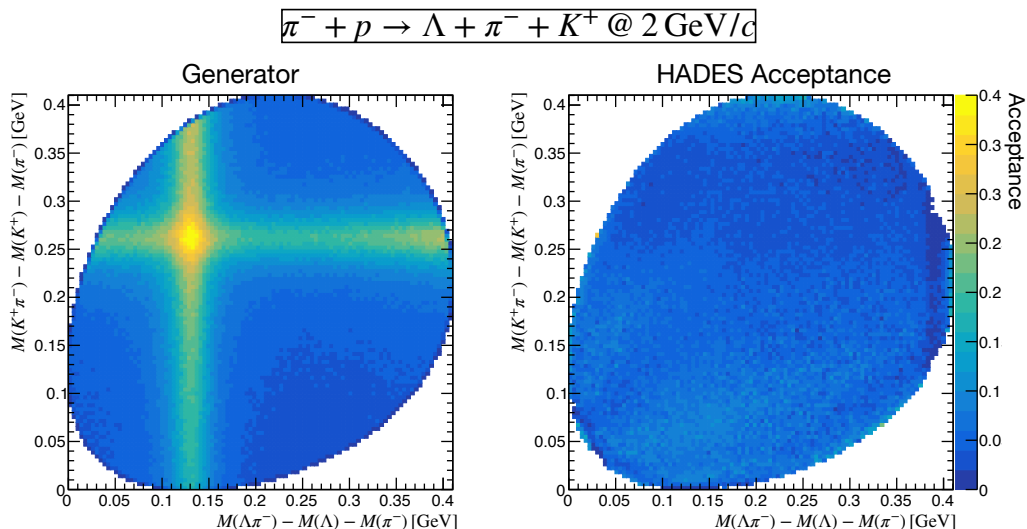


Figure 11: Pluto simulation of the reaction $\pi^- + p \rightarrow \Lambda + \pi^- + K^+$ with $\Lambda \rightarrow \pi^- p$. *Left panel:* The output of the generator which includes a incoherent sum of phase-space model plus a model incorporating two intermediate resonances, namely the $\Sigma(1385)$ and $K^*(892)$ resonances. *Right panel:* The acceptance of HADES for which all the final-state particles are registered by the HADES central detector or forward wall. Moreover, the momenta of all final-state particles are required to be larger than 100 MeV/c.

Figure 11 illustrates the mass correlation between the πK and $\pi\Lambda$ systems for the reaction $\pi^- + p \rightarrow \Lambda + \pi^- + K^+$ with $\Lambda \rightarrow p\pi^-$ at a pion-beam momentum of 2 GeV/c, based on a Pluto simulation. The generator incorporates a mixture of a phase-space model and models with intermediate states involving the $\Sigma(1385)$ and $K^*(892)$. The left panel displays the generated spectrum, while the right panel shows the HADES acceptance, where all final-state particles are detected. It is noteworthy that the setup provides nearly complete phase-space coverage of the reaction with a uniform acceptance.

5 Experimental set-up

5.1 The (upgraded) HADES facility

HADES is a charged-particle detector consisting of a 6-coil toroidal magnet centered around the beam axis and six identical detection sections located between the coils covering almost the full azimuthal angle. Each sector is equipped with a Ring- Imaging Cherenkov (RICH) detector followed by Mini- Drift Chambers (MDCs), two in front of and two behind the magnetic field, as well as a scintillator hodoscope (TOF) and a Resistive Plate Chamber (RPC). At the end of the system a forward hodoscope used for event plane determination is located. The RICH detector is used mainly for electron/positron identification, the MDCs are the main tracking detectors, while the TOF and RPC are used for time-of-flight measurements in combination with a diamond start-detector located in front of the 15-fold segmented target. The trigger is based on the hit multiplicity in the TOF covering a polar angle range between 45° and 85° . A detailed description of the HADES detector is given in [68].

The measurements we propose on baryonic resonances and cold hadronic matter will take advantage of foreseen improvements of the pion beam properties. In addition, the HADES set-up will comprise four new devices with respect to the former pion beam experiment in 2014:

- ▶ The new RICH photon detector, successfully operated already in the latest HADES experiments in 2019 and 2022, provides an increased electron reconstruction efficiency by about a factor 3.
- ▶ The ECAL, also used in 2019 and 2022, extends the capacity of HADES and provides high precision differential cross sections for hadronic channels to exit channels containing neutral mesons and photons.
- ▶ A new t0 and beam tracking detector based on Low Gain Avalanche Diode technology will be installed in front of the HADES target and will replace the Si tracker and diamond detector used in 2014. With three stations in front of the target, pion beam particles hitting the target can be selected and background rejected, hence providing a more accurate normalization of beam pions interacting with target nuclei. The trigger of the acquisition will be provided by a coincidence between a fast signal in the t0 detector and at least two signals in the RPCs or TOF-scintillators. This will induce no bias, since all the channels we want to measure have two charged particles in the final state.
- ▶ The new straw tube Forward Detector was already operated in 2022 and covers the angular range between 0.5 and 6° , which can be useful in particular for elastic scattering measurements, which are useful for the normalization using the existing EPECUR data [69] and for efficiency checks.

5.2 The GSI pion-beam facility

The GSI accelerator complex with a synchrotron of 18 Tm maximum rigidity delivers protons and ions up to beam energies of 4.5 GeV and 2 AGeV, respectively. A dedicated target station for the production of secondary beams has been built already in the nineties [REF] and serves several caves. The HADES experiment is connected via a beam line with a tilted dipole system (D1, D2) such as to elevate the standard beam tube height by 0.5 m up to the central axis of the spectrometer. The beam line is depicted in Fig. 12. The HADES target

point is located about 33.5 m downstream of the production target. Position sensitive beam tracking detectors C1 and C2 are mounted close to the intermediate focal planes between the two dipoles (C1) and between the quadrupoles inside the HADES cave (C2). These quadrupoles (Q7, Q8, Q9 with $\ell = 1$ m and $\ell = 0.4$ m) can be adjusted individually in position and are relevant for the focusing conditions at the HADES target point.

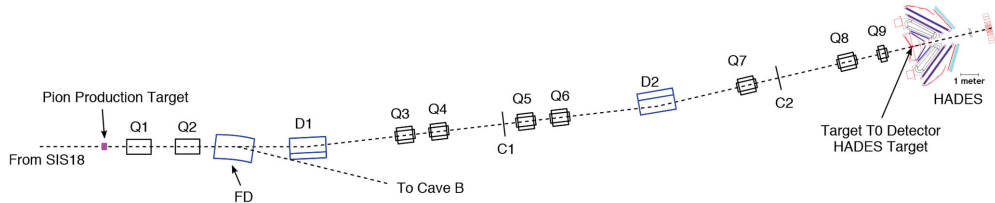


Figure 12: Schematic overview of the beam line between the pion production target and the HADES cave. The dipole magnets (D), quadrupoles (Q), tracking detectors (C1, C2) and the target T0 detector are included in the transport simulations. The FD dipole used to direct the beam to cave B is treated as a passive element. Figure is taken from [70].

The secondary pion beam is generated using an extracted primary ^{14}N beam at the highest possible intensity, impinging on a 10 cm-long beryllium target for all energies, except at the highest energy of $\sqrt{s} = 2.35$ GeV. At this energy, a primary proton beam impinging on beryllium is required to achieve sufficient intensity for the secondary pion beam.

The experiment in 2014 was realized using 36 shifts with an average of $2.2 \cdot 10^5$ pions per second on the HADES target produced by a primary beam intensity of 4×10^{10} nitrogen ion/s. We used moderate extraction times to realize a 30% duty cycle. This beam time estimate considers the following changes w.r.t. to the previous experiment. First, the flux of π^- with $p = 1.1$ GeV/c at the production target is a factor of two higher compared to π^- with momentum $p = 0.7$ GeV/c, due to the forward boost of the produced pions [70]. Second, an additional increase by a factor two is expected using the maximum SIS18 primary beam intensity of $7 \times 10^{10}/s$ and taking into account improvements of the slow beam extraction, and the shielding added in the extraction area. The pions in a selected momentum range (with a bandwidth of about 1.7% (*rms*)) are transported up to the HADES target by a set of nine quadrupoles and two dipoles. We will use five dipole settings to select different incident pion beam momenta, as explained below. The quadrupole settings will be adjusted according to second order beam optics calculations to optimize the acceptance and focus requirements of the pion beam line.

We will use five different targets: a polyethylene (CH_2) block with a length of 4.6 cm, a carbon (C) target consisting of 7 segments, each 3.6 mm long, and interspersed by 7.1 mm, a silver (Ag) target consisting of 15 segments, each 0.47 mm long and interspersed by about 3.6 mm and iron (Fe) and lead (Pb) targets each with thickness of 8 mm. All targets have the same 12 mm diameter. The choice of a polyethylene target is dictated by the larger density (factor 2) of protons ($3.8 \cdot 10^{23}/\text{cm}^2$) as compared to the one available in a LH_2 targets and the absence of background originating from interactions with the target vessel. The latter is unavoidable due to the pion beam diameter (FWHM $\sim 1.5 - 2$ cm) which exceeds the diameter of the LH_2 target. The C and Ag target are segmented to reduce the energy loss due to bremsstrahlung and the background due to conversion of real photons, which impact the quality of e^+e^- measurements. The effective luminosities, calculated using a duty factor $\varepsilon_{duty} = 0.5$ and a DAQ efficiency $\varepsilon_{LT} = 0.5$, amount for interactions with protons and carbon nuclei in the polyethylene target to $L_H^{eff} = 84.4$ and $42.2 \text{ mb}^{-1} \cdot s^{-1}$, respectively. For interactions in the carbon and silver targets the effective luminosities are

$L_C^{eff} = 58.4 \text{ mb}^{-1} \cdot \text{s}^{-1}$ and $L_{Ag}^{eff} = 8.05 \text{ mb}^{-1} \cdot \text{s}^{-1}$, respectively.

References

- [1] J. Adamczewski-Musch et al. Probing dense baryon-rich matter with virtual photons. *Nature Phys.*, 15(10):1040–1045, 2019.
- [2] R. Abou Yassine et al. First measurement of massive virtual photon emission from n^* baryon resonances, 2024.
- [3] G. Barucca et al. PANDA Phase One. *Eur. Phys. J. A*, 57(6):184, 2021.
- [4] M. Post, S. Leupold, and U. Mosel. Hadronic spectral functions in nuclear matter. *Nucl. Phys. A*, 741:81–148, 2004.
- [5] R. Nasseripour et al. Search for medium modification of the rho meson. *Phys. Rev. Lett.*, 99:262302, 2007.
- [6] M. Naruki et al. Experimental signature of the medium modification for rho and omega mesons in 12-GeV $p + A$ reactions. *Phys. Rev. Lett.*, 96:092301, 2006.
- [7] G. Agakishiev et al. First measurement of low momentum dielectrons radiated off cold nuclear matter. *Phys. Lett.*, B715:304–309, 2012.
- [8] M. Effenberger et al. $e^+ e^-$ pairs from $\pi^- A$ reactions reexamined. *Phys. Rev.*, C60:027601, 1999.
- [9] J. Adamczewski-Musch et al. Strong absorption of hadrons with hidden and open strangeness in nuclear matter. *Phys. Rev. Lett.*, 123(2):022002, 2019.
- [10] Fatima Hojei. Study of hadronic channels in the $\pi^- + C$ reaction at 0.69 GeV/c with HADES. PHD, Paris-Saclay university, 2023.
- [11] B. Ramstein. *EPJ Web Conf.*, 291:04004, 2024.
- [12] G. Ramalho and M. T. Pena. $\gamma^* N \rightarrow N(1520)$ form factors in the timelike regime. *Phys. Rev.*, D95(1):014003, 2017.
- [13] W. J. Briscoe et al. Physics opportunities with meson beams. *Eur. Phys. J.*, A51(10):129, 2015.
- [14] J. Adamczewski-Musch et al. Probing dense baryon-rich matter with virtual photons. *Nature Phys.*, 15(10):1040–1045, 2019.
- [15] J. Adamczewski-Musch et al. Two-Pion production in the second resonance region in $\pi^- p$ collisions with HADES, 2020.
- [16] R. Abou Yassine et al. Inclusive e^+e^- production in collisions of pions with protons and nuclei in the second resonance region of baryons, 2023.
- [17] V. I. Mokeev et al. Evidence for the $N'(1720)3/2^+$ Nucleon Resonance from Combined Studies of CLAS $\pi^+ \pi^- p$ Photo- and Electroproduction Data. *Phys. Lett.*, B805:135457, 2020.
- [18] B. W. Allardyce et al. Pion reaction cross-sections and nuclear sizes. *Nucl. Phys.*, A209:1–51, 1973.

- [19] G. Agakishiev et al. Baryon resonance production and dielectron decays in proton-proton collisions at 3.5 GeV. *Eur. Phys. J.*, A50:82, 2014.
- [20] J. Adamczewski-Musch et al. Analysis of the exclusive final state npe^+e^- in quasi-free np reaction. *Eur. Phys. J.*, A53(7):149, 2017.
- [21] J. Adamczewski-Musch et al. $\Delta(1232)$ Dalitz decay in proton-proton collisions at $T=1.25$ GeV measured with HADES at GSI. *Phys. Rev.*, C95(6):065205, 2017.
- [22] G. Ramalho and M. T. Pena. Covariant model for the Dalitz decay of the $N(1535)$ resonance. arXiv:2003.04850[hep-ph], 2020.
- [23] M. F. M. Lutz, B. Friman, and M. Soyeur. Quantum interference of rho0 and omega-mesons in the $\pi N \rightarrow e^+e^- N$ reaction. *Nucl. Phys.*, A713:97–118, 2003.
- [24] E. Speranza, M. Zetenyi, and B. Friman. Polarization and dilepton anisotropy in pion-nucleon collisions. *Phys. Lett.*, B764:282–288, 2017.
- [25] A. Baldini, V. Flaminio, W.G. Moorhead, D. R.O. Morrison, and H. (Ed) Schopper. Numerical data and functional relationships in science and technology. GRP. 1: Nuclear and particle physics. Vol. 12. *Landolt Börnstein new series*, 1988.
- [26] V. Shklyar, H. Lenske, and U. Mosel. Eta-meson production in the resonance energy region. *Phys.Rev.*, C87:015201, 2013.
- [27] M. Effenberger, E. L. Bratkovskaya, and U. Mosel. $e^+ e^-$ pair production from gamma A reactions. *Phys. Rev.*, C60:044614, 1999.
- [28] H. Karami et al. *Nucl. Phys.*, B154:503–518, 1979.
- [29] A. I. Titov and B. Kämpfer. Isoscalar-Isovector Interferences in $\pi N \rightarrow Ne^+e^-$ Reactions as a Probe of Baryon Resonance Dynamics. *Eur. Phys. J.*, A12:217–229, 2001.
- [30] G. Ramalho and Teresa Pena. *Prog. Part. Nucl. Phys.*, 136:104097, 2024.
- [31] M. Zetenyi et al. *Phys. Rev.*, C104:015201, 2021.
- [32] Luis Alvarez-Ruso Fernando Alvarado, Di An and Stefan Leupold. *Phys. Rev.*, D108:11, 2023.
- [33] Di An and Stefan Leupold. Electromagnetic isovector form factors of the transition from the $n^*(1520)$ to the nucleon, 2024.
- [34] R. Kaminski et al. *Phys. Rev. D*, 77:054015, 2008.
- [35] R. Kaminski et al. *Phys. Rev. D*, 83:076008, 2011.
- [36] R. Garcia-Martin et al. *Phys. Rev. Lett.*, 107:072001, 2011.
- [37] A. Alavi-Harati et al. *Phys. Rev. Lett.*, 84:408, 2000.
- [38] A. Lai et al. *Eur. Phys. J.*, C30:33, 2003.
- [39] K. Abe et al. *Phys. Lett.*, B517:309, 2001.
- [40] B. Aubert et al. *Phys. Rev. Lett.*, 86:2515, 2001.

-
- [41] B. H. Behrens et al. *Phys. Rev. Lett.*, 80:3710, 1998.
- [42] T. E. Browder et al. *Phys. Rev. Lett.*, 81:1786, 1998.
- [43] S. J. Richichi et al. *Phys. Rev. Lett.*, 85:520, 2000.
- [44] R. J. Crewther et al. *Phys. Lett.*, B88:123, 1980.
- [45] J. M. Pendlebury et al. *Phys. Rev.*, D92:092003, 2015.
- [46] D. S. M. Alves. *Phys. Rev.*, D103:055018, 2021.
- [47] N. A. Weiner D. S. M. Alves. *J. High Energ. Phys.*, 92, 2018.
- [48] S. Gonzalez-Solis D. S. M. Alves. *J. High Energ. Phys.*, 07:264, 2024.
- [49] A. J. Krasznahorkay et al. *Phys. Rev. Lett.*, 116:042501, 2016.
- [50] A. J. Krasznahorkay et al. *arXiv:1910.10459*.
- [51] T. A. DeGrand and H. I. Miettinen. *Phys. Rev.*, D23:1227, 1981.
- [52] T. A. DeGrand and H. I. Miettinen. *Phys. Rev.*, D24:2419, 1985.
- [53] R. D. Baker et al. *Nucl. Phys.*, B141:29, 1978.
- [54] R. L. Crollius et al. . *Phys. Rev.*, 155:1455, 1967.
- [55] G. Penner and U. Mosel. . *Phys. Rev.*, C66:055212, 2002.
- [56] K. H. Hicks and H. Sako. J-PARC Proposal E45, Japan.
- [57] K. Miwa et al. J-PARC Proposal P86, Japan.
- [58] Y. Wunderlich A. Thiel, F. Afzal. Light Baryon Spectroscopy. *Prog. in Part. and Nucl. Phys.*, 125:103949, 2022.
- [59] M. Ablikim et al. *Nat. Phys.*, 15:631, 2019.
- [60] Apiwit Kittiratpattana, Tom Reichert, Nihal Buyukcizmeci, Alexander Botvina, Ayut Limphirat, Christoph Herold, Jan Steinheimer, and Marcus Bleicher. Production of nuclei and hypernuclei in pion-induced reactions near threshold energies. *Phys. Rev. C*, 109(4):044913, 2024.
- [61] S. Spies. Strange Hadron Production in Ag+Ag Collisions at 1.58A GeV. *PhD Thesis*, Goethe-University Frankfurt, 2022.
- [62] A. D. Sakharov. *Zh. Eksp. Teor. Fiz. Pisma*, 5:32, 1967.
- [63] J. F. Donoghue and S. Pakvasa. *Phys. Rev. Lett.*, 55:162, 1985.
- [64] *Phys. Rev. Lett.*, 93:262001, 2004.
- [65] Elisabetta Perotti, Göran Fäldt, Andrzej Kupsc, Stefan Leupold, and Jiao Jiao Song. Polarization observables in e^+e^- annihilation to a baryon-antibaryon pair. *Phys. Rev. D*, 99(5):056008, 2019.
- [66] M. Ablikim et al. *Nature (London)*, 606:64, 2022.

- [67] M. Ablikim et al. *Phys. Rev. Lett.*, 132:101801, 2024.
- [68] G. Agakichiev et al. The high-acceptance dielectron spectrometer hades. *The European Physical Journal A*, 41(2):243–277, July 2009.
- [69] A. Gridnev et al. Search for narrow resonances in πp elastic scattering from the EPECUR experiment. *Phys. Rev.*, C93(6):062201, 2016.
- [70] J. Diaz et al. Design and commissioning of the GSI pion beam. *Nucl. Instrum. Meth.*, A478:511–526, 2002.

6 Submitted proposals GPAC 2025

G_24_00209: 105 shifts

“Electromagnetic baryon transition form factor in the third resonance region.”

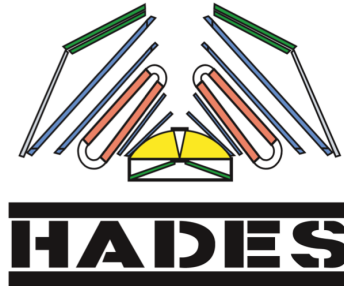
G_24_00255: 66 shifts

“Energy scan of the third baryon resonance region and hyperon polarization.”

ELECTROMAGNETIC BARYON TRANSITION FORM FACTOR IN THE THIRD RESONANCE REGION

Pion induced reactions on CH₂ and C targets

The HADES Collaboration



Spokespersons: J. Stroth (j.stroth@gsi.de), P. Tlustý (tlusty@ujf.cas.cz)
GSI contact: J. Pietraszko (j.pietraszko@gsi.de)

Infrastructure: SIS18, pion production target and HADES cave
Beam: Nitrogen at 2A GeV, maximum intensity, slow extraction

Abstract

This is a resubmission of a part of the proposal G-22-00141. The proposed experiment addresses the electromagnetic transitions of baryon resonances in the third resonance region. The proposal is based on the successful extraction of the dielectron invariant mass distribution from Dalitz decays of baryon resonances in the second resonance region as demonstrated in an earlier experiment with conducted in 2014 with a pion beam directed at the HADES spectrometer. The dielectron invariant mass distribution obtained from the analysis of the electromagnetic transition of the reaction $\pi^- + p \rightarrow n + e^+ + e^-$ showed strong evidence for the formation of intermediary ρ mesons mediating the decay into a pair of electrons. We expect an even stronger effect in the third resonance region due to the larger Q value of the resonance decay ($Q \simeq m_\rho$) and consequently a stronger sensitivity in the discrimination of respective model calculations. The reconstructed phase space distributions and spin-density matrices for various channels will be used as input to partial wave analyses to extract the dominant amplitudes contributing to the decay into two pions plus nucleon final states. Further input to the partial wave analysis will come from a measurement of hadronic final states in a resonance scan addressing also energies slightly below and above the central energy proposed here (*cf.* G-24-00255). Compared to the situation in 2014, when radiation issues were restricting the intensity of the primary beam, meanwhile the ACC division has successfully slow-extracted a ^{14}N beam of 7×10^{10} ions and directed to the pion production target located down stream the HETB without surpassing critical radiation levels. The original proposal G-22-0141 was granted 95 shifts but a A^- rating because at the time, the availability of high-intensity secondary pion beams had not been established.

This is a re-submission of of part of G-22-0141

We request 105 shifts.

ELECTROMAGNETIC BARYON TRANSITION FORM FACTOR IN THE THIRD RESONANCE REGION

Pion induced reactions on CH₂ and C targets

The HADES Collaboration

This proposal asks for 105 shifts of primary ¹⁴N beam

State of the art

Pion beam experiments in the 0.5-2.5 GeV/c momentum range are an essential component of the program of dense matter studies pursued by HADES at SIS18 and the future Compressed Baryonic Matter pillar at FAIR. They provide unique information on the role of baryonic resonances in the production of mesons and dielectrons, both in vacuum and in medium. There are a central motivation for pion beam experiments in the SIS18 energy range but also address fundamental aspects of the structure of baryons.

Baryon-meson couplings

Together with photon-nucleon reactions, pion-nucleon reactions provide direct information on the electromagnetic and hadronic couplings of baryonic resonances, which are related to their intrinsic structure in terms of quarks and gluons through hadron-structure models and provide important constraints for cross sections used in microscopic transport simulations. While the data base for photon-induced reactions has been continuously developed in the past years, the progress in the determination of the baryon spectrum and related decay properties is currently limited by the lack of precise data from pion-beam experiments [1]. HADES is at this moment the only facility world-wide which combines a pion beam with dielectron spectroscopy, an excellent particle identification and good secondary vertex reconstruction capabilities [2]. The pion beam program we want to pursue at GSI is documented in the white paper π -QCD [3] and complements activities at existing and future meson beam facilities for baryon spectroscopy [1, 4].

A better determination of the couplings of baryonic resonances to ρ N and ω N final states is particularly important for the understanding of the emissivity of hot and dense nuclear matter due to the important role of intermediary vector mesons in dilepton emission. In particular baryon- ρ interactions are the origin of significant melting in of the ρ meson in model calculations of the emissivity of hadronic matter formed in heavy-ion collisions from SIS18 to LHC energies [5]. The physics potential of pion-induced reactions combined with HADES, particularly for cross-community applications, has been unequivocally demonstrated in previous studies. A notable example is the investigation of the $N^*(1520) \rightarrow Ne^+e^-$ electromagnetic transition form factor (emTFF) in $\pi^-p \rightarrow Ne^+e^-$ at a centre-of-mass energy of $\sqrt{s} = 1.5$ GeV. The q^2 dependence of the emTFF, together with a partial wave analysis (PWA) of simultaneously reconstructed $\pi^-p \rightarrow \pi^+\pi^-n$ data, provided a microscopic study of the electromagnetic structure and hadronic properties of baryonic transitions, such as the validity of vector-meson dominance and the role of pion clouds. This information is crucial for understanding e^+e^- mass spectra in $A + A$ reactions, especially in the context of the ρ contribution melting in baryon-dense environments and simultaneously provides new insights into our understanding of baryon resonances and their decays.

Electromagnetic Baryon Transitions in the time-like regime

HADES experiments performed in the last years in proton-nucleus [6] or nucleus-nucleus [5] reactions have demonstrated an excess radiation of e^+e^- above conventional sources. The excess radiation measured by HADES in heavy-ion collisions is clearly attributed to emission out of the hot and dense stage of the reaction (fireball) [5]. The most successful explanation is that this radiation emerges from decays of far off-shell ρ mesons with a strongly modified spectral function due to their coupling to baryonic resonances in hadronic matter. The study of elementary reactions, like p+p, quasi-free n+p and π^-+p [7, 8, 9, 10] provided an important reference for the excess determination. Support for the importance of intermediary ρ mesons in a

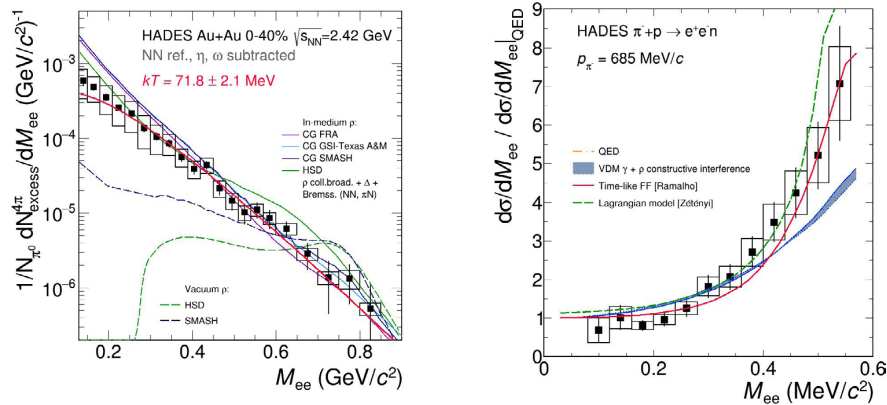


Figure 1: Left: Dilepton excess yield in the low invariant mass region for Au+Au collisions at 2.42 GeV compared to various model predictions [5]. A fit of a Planck distribution works well and suggests that the distribution is of thermal origin. Right: Invariant mass of pairs from $N^* \rightarrow N\gamma^* \rightarrow Ne^+e^-$ normalised by QED prediction for point-like transitions [HADES, arXiv:2205.15914]. Figure taken from NuPECC long-range plan 2024.

baryon-photon coupling was first provided by a measurements of resonance Dalitz decays ($N/\Delta \rightarrow Ne^+e^-$), in accordance with the Vector Dominance Model (VMD) [9, 10]. This observation has recently been substantiated by the results of a first pioneering experiment using π^- beam performed in 2014 using polyethylene and carbon targets. The invariant mass distribution for the the $\pi^-+p \rightarrow ne^+e^-$ channel is shown in the right panel of Fig. 1. A significant rise of the transition strength above the expectation for a point-like (QED) transition is observed for higher invariant masses, i.e. when approaching the free ρ pole mass. However, due to the Q value of the resonance decay, the phase space for the dielectron cuts of about 200 MeV before.

Pion beam experiments provide an increased sensitivity to these effects, as the resonances are excited in the s-channel in a narrow mass bin, corresponding to the pion beam momentum dispersion. This limits the overlap between many baryon states, which is unavoidable in the case of nucleon-nucleon reactions. This information is complementary to the one obtained in electron scattering experiments in the space like region ($q^2 < 0$) and is therefore needed for a global understanding of these transitions. The differential cross sections in the $\pi^-+p \rightarrow ne^+e^-$ reaction can be parameterized in a model independent way using different equivalent functions (helicity amplitudes, form factors or spin density matrix elements), which contain information on the electromagnetic structure of the baryon transitions. This information will substantially contribute to the understanding of the the structure of excited baryon states. In particular, in the context of the HADES heavy-ion program, the interest of studying the $\pi^-+p \rightarrow ne^+e^-$ reaction is to scrutinize understanding of the coupling to lepton pairs, which is a key element for using virtual photon radiation to probe QCD matter under extreme conditions.

Expected results

The HADES collaboration has previously provided results on baryon electromagnetic transition form factors in the time-like domain and interpreted dilepton excess radiation as thermal radiation from hadronic matter. We aim to exploit pion interactions to deliver selective, novel insights into the unexplored third resonance region. With sufficient centre-of-mass energy for associate strangeness production, the data will allow detailed studies of strangeness phase space distribution and polarization. This proposal focuses on a long run at fixed pion beam momentum to collect significant data on resonance electromagnetic decay, complemented in proposal G-24-00255 by a five-step energy scan around the central energy, targeting hadronic final states. For further details, see our White Paper [3]. In a 2014 experiment, we measured e^+e^- production from polyethylene and carbon targets at a πN centre-of-mass energy of $\sqrt{s}=1.49$ GeV, near the $N(1520)$ resonance pole. Insufficient e^+e^- event statistics on the carbon target prevented accurate subtraction to isolate π^-+p interactions, but the quasi-free nature of e^+e^- production in the π^-+C reaction was confirmed and incorporated into a quasi-free participant-spectator model for the π^-+CH_2 reaction [10].

The expected M_{ee} invariant mass distributions for the $\pi^-+p \rightarrow n e^+e^-$ channel can be estimated from the known $\gamma n \leftrightarrow \pi^-+p$ cross-sections in a simple QED calculation, assuming a point-like vertex. To estimate the

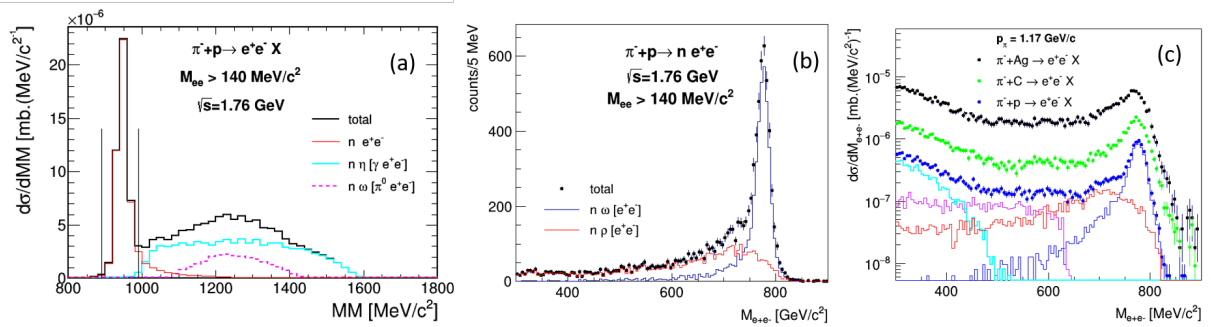


Figure 2: Simulations of the reaction $\pi^- p \rightarrow X e^+ e^-$ at $p_\pi = 1.16$ GeV/c including all known sources of dileptons. (a) Missing mass (M_{miss}) distribution for events with invariant mass $M_{ee} > 140$ MeV/ c^2 . (b) Expected distribution of counts in 5 MeV bins as a function of the invariant mass after selection of the exclusive channel using the condition on the missing mass $0.9 < M_{\text{miss}} < 1.03$ GeV/ c^2 . (c) Expected reconstructed inclusive $e^+ e^-$ invariant mass spectra for measurements on the silver target (black dots), carbon target (green dots) and for interaction with protons in the polyethylene targets (blue dots). The cyan, violet, red and blue curves display the $\eta \rightarrow e^+ e^-$, $\omega \rightarrow \pi^0 e^+ e^-$, $\rho \rightarrow e^+ e^-$ and $\omega \rightarrow e^+ e^-$ contributions.

effect of time-like electromagnetic transition form factors (etff), which are expected to modify the yield at large M_{ee} , we used models recently developed for the N-N(1520) [11] and N-N(1535) [12, 13] transitions. In this model, the baryon-photon interaction comprises both a coupling to the quark core and to the meson cloud, with parameters fitted to existing data in the space-like region. The coupling to the meson cloud causes a significant enhancement of the dielectron yield at large M_{ee} w.r.t. QED calculations and provide a quantitative description of HADES data.

To demonstrate the feasibility of the measurement at higher energy, we developed full scale simulations of the $\pi^- p \rightarrow X e^+ e^-$ reaction. For the Dalitz decays of π^0 and η mesons ($\pi^0, \eta \rightarrow \gamma e^+ e^-$), which constitute the dominant contributions, the production cross sections from previous experiments were used [14, 15]. Di-electron emission from intermediate $\Delta(1232)$ Dalitz decay ($\Delta(1232) \rightarrow N e^+ e^-$) is also taken into account, using $\Delta\pi$ cross sections from a Bonn-Gatchina PWA solution of the $\pi^- p$ reaction, but has a much smaller contribution. For the simulation of the $\pi^- p \rightarrow n e^+ e^-$ exclusive channels considered here as our signal, we used the two-component approach, which was successful for the data in the second resonance region, as described above. Following the analysis of the $\pi^- p \rightarrow n\gamma$ reaction around $\sqrt{s} = 1.76$ GeV, the N(1675) and $\Delta(1700)$ baryon resonances were identified as providing the most important contributions, due to their large γN couplings. The ρ production cross sections is taken from the HSD model [16] (2.1 mb at $\sqrt{s} = 1.76$ GeV), which accounts for the coupling of the ρ meson to baryon resonances. The higher (30 %) branching ratio for ρ to $e^+ e^-$ of $6 \cdot 10^{-5}$ w.r.t. the one at the pole is due to the enhanced production of low-mass ρ mesons due to the coupling to baryons. These values depend strongly on baryon resonance couplings to the ρN channel, which will be extracted from a PWA of $\pi^+ \pi^- n$ and $\pi^0 \pi^- p$. For $\pi^- p \rightarrow \omega n$, we used measured cross sections (10% precision) from Rutherford Laboratory [17], as the ω spectral function is less sensitive to baryon coupling. For the combined acceptance and reconstruction efficiency of $e^+ e^-$ pairs produced from ρ and ω , we find values of 25% and 31% respectively from GEANT simulations, taking into account in particular the improved efficiency of the $e^+ e^-$ pair reconstruction provided by the new photon detector of RICH. First, we demonstrate on Fig. 2(a) the capacity to select the exclusive channel $\pi^- p \rightarrow n e^+ e^-$ using the missing mass technique. The only significant source of uncertainty in the simulations of the background channels is related to the πN bremsstrahlung contribution $\pi N \rightarrow \pi N e^+ e^-$ (not included), which should however be easily separated from our signal using missing mass selection. In addition, no significant contribution of this type could be observed at $\sqrt{s} = 1.49$ GeV. The $e^+ e^-$ invariant mass distribution for the exclusive channel is displayed in Fig. 2(b). The ρ meson contribution is shown to span over a broad invariant mass range below the pole. As the ρ meson mass distribution, including the contributions of the different baryon resonances will also be extracted from the PWA of the two-pion production channels, a direct check of the Vector Dominance Mode will be possible, in a much broader range than in our previous experiment, where the invariant mass distribution was limited to about 550 MeV/ c^2 . The choice of a centre-of-mass energy 40 MeV above the ω production threshold allows for a detailed study of the ω meson spectral function, which will serve as a reference for studies of omega absorption in nuclei which will be subject of a further proposal not submitted this time. In the region below the ω peak, significant interferences between the

isoscalar ("ρ-like") and the isovector ("ω-like") e^+e^- productions might be present, as predicted by [18, 19] and could be studied as well.

Experimental set-up

We describe here only changes relative to the beam time taken in 2022. The forward detectors (**FD**), including the straw tracking stations and the forward RPC, will not be used for this run. The **ECAL** has now all six sectors equipped and provides independent measurement of neutral meson production. A **T0** detector based on Low Gain Avalanche Diode or on scCVD diamond technology will be installed in front of the HADES target with similar geometries as used in 2014. The **MDC** will be operated with the new front-end electronics providing multi-hit capability and a reduced dead time.

The secondary pion beam is produced using an extracted primary ^{14}N beam at the highest possible intensity impinging on a 10 cm long beryllium target. In a test beam time conducted by Accelerator division it was demonstrated, that a ^{14}N beam of 7×10^7 ions per spill and at maximum rigidity could be slow-extracted to the pion production target without surpassing safety radiation levels. The spill length will be set such as to not go below a duty cycle of 50%. The exact value will depend on the spill shape and on the fill and acceleration time. Comparing to the performance in 2014, we expect about 800.000 π^- per spill impinging on our target.

Justification of the beam time

Our first goal is to obtain for the invariant mass distributions in the $\pi^- + p \rightarrow n e^+ e^-$ channel statistical errors after carbon subtraction of interactions with carbon nuclei more than a factor 10 lower than in the previous experiment. For this, larger statistics both on the polyethylene and carbon target is needed. Events on the carbon target will be also used to check in detail the validity of the quasi-free assumption and estimate nuclear effects. In addition, we need more than 5000 quasi-free events measured on carbon and polyethylene targets for the analysis of the angular distributions and the extraction of the spin density matrix elements, in three M_{ee} bins ([300–550], [550–700] and [700–900] MeV/ c^2). Both requirements can be achieved with the following runs:

- ▶ at $\sqrt{s} = 1.76$ GeV: 56 shifts on the polyethylene target and 43 shifts on the carbon target
- ▶ 6 shifts for tuning and calibration and accounting for the target changes. In particular, the alignment of the primary beam on the pion production target and of the pion beam on the t0 detector in front of the target needs careful adjustments of the corresponding dipoles.

At the time of this proposal a concept nor a proof for a knock-out extraction using a feed-back signal from the experiment was not established for high-intensity beam. This beam time estimate considers the following changes w.r.t. to the 2014 pion beam experiment. First, the flux of π^- with $p = 1.1$ GeV/ c at the production target is a factor of two higher compared to π^- with momentum $p = 0.7$ GeV/ c , due to the forward boost of the produced pions [20]. Second, an additional increase by a factor two is expected using the maximum SIS18 primary beam intensity of $7 \cdot 10^{10}/s$ as it has been demonstrated in a beam test in November 2023. We will use two different targets: a polyethylene (CH_2) block with a length of 4.6 cm and a carbon (C) target consisting of 7 segments, each 3.6 mm long. The choice of a polyethylene target is dictated by the fact that the pion beam transverse distribution (FWHM $\sim 1.5 - 2$ cm) reaches significantly to outside of the aperture of the LH_2 target. The C is segmented to reduce the energy loss due to bremsstrahlung and the background due to conversion of real photons. The effective luminosities, calculated using a duty factor $\varepsilon_{duty} = 0.5$ and a DAQ efficiency $\varepsilon_{LT} = 0.5$, amounts for interactions with protons and carbon nuclei in the polyethylene target to $L_H^{eff} = 84.4$ and $42.2 \text{ mb}^{-1} \cdot s^{-1}$, respectively. For interactions in the carbon target the effective luminosity is $L_C^{eff} = 58.4 \text{ mb}^{-1} \cdot s^{-1}$. These considerations are also valid for the proposal G-24-00255.

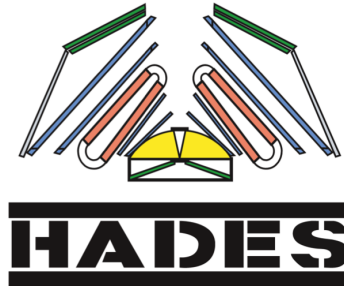
Bibliography

- [1] W. J. Briscoe et al. Physics opportunities with meson beams. *Eur. Phys. J.*, A51(10):129, 2015.
- [2] J. Adamczewski-Musch et al. A facility for pion-induced nuclear reaction studies with HADES. *Eur. Phys. J. A*, 53(9):188, 2017.
- [3] HADES Collaboration. π -QCD - proposal for experiments at the gsi pion beam facility. https://hades.gsi.de/sites/default/files/web/media/documents/proposals/HADES_Proposal_Pion_TitlePage-only.pdf.
- [4] K. H. Hicks and H. Sako. J-PARC Proposal E45, Japan, 2012; <http://www.phy.ohiou.edu/~hicks/NSF/2013/JPARC-P45.pdf>.
- [5] J. Adamczewski-Musch et al. Probing dense baryon-rich matter with virtual photons. *Nature Phys.*, 15(10):1040–1045, 2019.
- [6] G. Agakishiev et al. First measurement of low momentum dielectrons radiated off cold nuclear matter. *Phys. Lett.*, B715:304–309, 2012.
- [7] G. Agakishiev et al. Baryon resonance production and dielectron decays in proton-proton collisions at 3.5 GeV. *Eur. Phys. J.*, A50:82, 2014.
- [8] J. Adamczewski-Musch et al. Analysis of the exclusive final state npe^+e^- in quasi-free np reaction. *Eur. Phys. J.*, A53(7):149, 2017.
- [9] J. Adamczewski-Musch et al. $\Delta(1232)$ Dalitz decay in proton-proton collisions at $T=1.25$ GeV measured with HADES at GSI. *Phys. Rev.*, C95(6):065205, 2017.
- [10] R. Abou Yassine et al. First measurement of massive virtual photon emission from n^* baryon resonances. *sub. to PRL*, arXiv:2205.15914, 2024.
- [11] G. Ramalho and M. T. Pena. $\gamma^*N \rightarrow N(1520)$ form factors in the timelike regime. *Phys. Rev.*, D95(1):014003, 2017.
- [12] G. Ramalho and M. T. Pena. Covariant model for the Dalitz decay of the $N(1535)$ resonance. *Phys. Rev.*, D101:114008, 2020.
- [13] G. Ramalho and Teresa Pena. *Prog. Part. Nucl. Phys.*, 136:104097, 2024.
- [14] A. Baldini, V. Flaminio, W.G. Moorhead, D. R.O. Morrison, and H. (Ed) Schopper. Numerical data and functional relationships in science and technology. GRP. 1: Nuclear and particle physics. Vol. 12. *Landolt Börnstein new series*, 1988.
- [15] V. Shklyar, H. Lenske, and U. Mosel. Eta-meson production in the resonance energy region. *Phys.Rev.*, C87:015201, 2013.
- [16] M. Effenberger, E. L. Bratkovskaya, and U. Mosel. e^+e^- pair production from gamma A reactions. *Phys. Rev.*, C60:044614, 1999.
- [17] H. Karami et al. elastic scattering and omega meson production near the threshold of $\pi^-p \rightarrow \omega n$. *Nucl. Phys.*, B154:503–518, 1979.
- [18] A. I. Titov and B. Kämpfer. Isoscalar-Isovector Interferences in $\pi N \rightarrow Ne^+e^-$ Reactions as a Probe of Baryon Resonance Dynamics. *Eur. Phys. J.*, A12:217–229, 2001.
- [19] M. F. M. Lutz, B. Friman, and M. Soyeur. Quantum interference of rho0 and omega-mesons in the $\pi N \rightarrow e^+e^- N$ reaction. *Nucl. Phys.*, A713:97–118, 2003.
- [20] J. Diaz et al. Design and commissioning of the GSI pion beam. *Nucl. Instrum. Meth.*, A478:511–526, 2002.

ENERGY SCAN OF THE THIRD BARYON RESONANCE REGION AND HYPERON POLARIZATION

Pion induced reactions on CH_2 and C targets

The HADES Collaboration



Spokespersons: J. Stroth (j.stroth@gsi.de), P. Tlusty (tlusty@ujf.cas.cz)
GSI contact: J. Pietraszko (j.pietraszko@gsi.de)

Infrastructure: SIS18, pion production target and HADES cave
Beam: Nitrogen at 2A GeV, maximum intensity, slow extraction

Abstract

This proposed experiment is partly a resubmission of G-122-00141, with an expanded scope motivated by results from previous data analyses. We aim to combine the resonance scan in the third resonance region, focusing on hadronic final states, with a comprehensive investigation of hyperon production and polarization observables. The study of two-pion final states at five distinct energies will play a pivotal role in improving partial wave analyses within this resonance region. The world database on Λ and Σ^0 polarization measurements will be significantly improved in terms of accuracy.

In 2022, we submitted a request for 143 shifts of pion beam time and received approval for 95 A^- shifts, which could not be scheduled. Although the scientific interest of the proposed measurements was recognized by the G-PAC, the experiment was not ranked due to required improvements in the accelerator to provide the desired beam quality.

This is re-submission in part of proposal G-22-00141

We request 66 shifts.

State of the art

Pion beam experiments in the 0.5–2.5 GeV/c momentum range are an essential component of the program of dense matter studies pursued by HADES at SIS18 and the future Compressed Baryonic Matter pillar at FAIR. They provide unique information on the role of baryonic resonances in the production of mesons and dielectrons, both in vacuum and in medium. The proposed pion-beam experiments are driven by several QCD-driven aspects in the non-perturbative regime, intimately connecting facets between hadron and heavy-ion physics. Together with photon-nucleon reactions, pion-nucleon reactions provide direct information on the electromagnetic and hadronic couplings of baryonic resonances, which are related to their intrinsic structure in terms of quarks and gluons through hadron-structure models.

While the data base for photon-induced reactions has been continuously developed in the past years, the progress in the determination of the baryon spectrum and related decay properties is currently limited by the lack of precise data from pion beam experiments [1]. A more precise determination of the couplings of baryonic resonances to ρN and ωN final states is particularly important for the understanding of the emissivity of hot and dense nuclear matter due to the important role of intermediary vector mesons in dilepton emission. In particular baryon- ρ interactions are known to strongly contribute to the observed melting of the ρ meson in the fireball formed in heavy-ion collisions from SIS18 to LHC energies [2]. A detailed understanding of these effects requires microscopic calculations which rely on these couplings.

In a first pion beam experiment in 2014, we measured the double pion production in the second resonance region ($\sqrt{s} \simeq 1.49$ GeV [3]). The obtained two-pion ($\pi^+\pi^-$ and $\pi^-\pi^0$) data samples have been included in the multichannel Partial Wave Analysis (PWA) of Bonn-Gatchina together with other world data on single and double pion production in photon, pion and electron induced reactions. This allowed for the identification of the various final ($\Delta\pi, \rho\pi, N\sigma$) and initial ($\frac{1}{2}^+, \frac{1}{2}^-, \frac{3}{2}^+, \dots$) resonant and non-resonant states. As the information on $\pi^+\pi^-$ and $\pi^-\pi^0$ channels from other experiments only exist as total cross sections, the HADES data were essential to constrain the ρ production (Fig. 2). We successfully *e.g.* extracted the branching ratios of the N(1440), N(1520) and N(1535) baryon resonances to the ρN channel, basic information which is presently absent in the Review of Particle Physics. This information has then been used for the interpretation of the dielectron production [4, 5] by means of the Vector Dominance Model.

We take these results as a proof of concept for the PWA method applied to HADES pion-beam data in the two-pion production channels. This approach can be readily extended to other hadronic channels in the third resonance region, including final states involving flavour SU(3) degrees of freedom, such as those with strangeness. At a centre-of-mass energy \sqrt{s} around 1.73 GeV, many hadronic channels are open (*e.g.* $K^0\Lambda$, $\Sigma^0 K^0$, $\Sigma^+ K^-$, ηn , ωn , ...) in addition to the two-pion production (see Fig. 1). These channels will help to constrain hadronic couplings of baryon states in this region ($\Delta(1620)$ $1/2^-$, $\Delta(1700)$ $3/2^-$, N(1650) $1/2^-$, N(1675) $5/2^-$, N(1680) $5/2^+$, N(1710) $1/2^+$, N(1720) $3/2^+$, ...) which are very poorly known. Our goal will therefore be to provide statistically-unprecedented differential data for hadronic channels, including those with neutral mesons. Together with complementary photo-production data, taken in a similar centre-of-mass energy at CBELSA, a combined effort with our close colleagues both from experiment and theory, *e.g.* Bonn-Gatchina

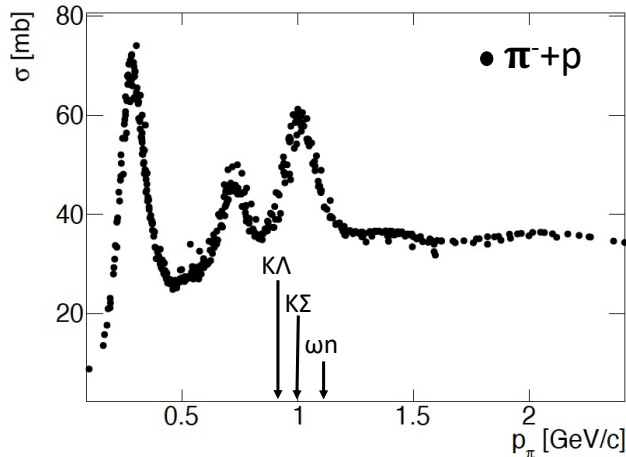


Figure 1: $\pi^- + p$ cross sections showing the three peaks corresponding to the $\Delta(1232)$, the second and third resonance regions, respectively. The black arrows indicate the thresholds for various hadronic final states.

channel	ε_{AR}	σ_H (mb)	σ_C (mb)	BR	C ₂ H ₄ target		C target
					\dot{N}_H/N_{tot} (shift ⁻¹)	\dot{N}_C (shift ⁻¹)	
$\pi^- \pi^+ n$	0.14	10	16	1	$3.4 \times 10^6 / 6.1 \times 10^6$	3.8×10^6	3.8×10^6
$\pi^- \pi^0 p$	0.09	6.5	10.4	1	$1.4 \times 10^6 / 2.6 \times 10^6$	1.6×10^6	1.6×10^6
$\pi^0 \pi^0 n$	0.01	2	3.2	1	$4.9 \times 10^4 / 8.8 \times 10^4$	5.4×10^4	5.4×10^4
$K^0 \Lambda$	0.04	0.56	1.85	0.35	$1.9 \times 10^4 / 5.0 \times 10^4$	4.3×10^4	4.3×10^4
$K^0 \Sigma^0$	0.04	0.24	0.79	0.35	$8 \times 10^3 / 2.2 \times 10^4$	1.9×10^4	1.9×10^4
$K^+ \Sigma^-$	0.13	0.23	0.76	1	$7.2 \times 10^4 / 1.9 \times 10^5$	1.7×10^5	1.7×10^5
ηn	0.01	1.2	3.96	0.39	$1.2 \times 10^4 / 3.1 \times 10^4$	2.6×10^4	2.6×10^4
ωn	0.015	1.5	4.95	0.89	$4.9 \times 10^4 / 1.3 \times 10^5$	1.1×10^5	1.1×10^5
$\rho \rightarrow e^+ e^-$	0.25	2.1	6.93	$6 \cdot 10^{-5}$	78/204	176	176
$\omega \rightarrow e^+ e^-$	0.31	1.7	5.61	$7.4 \cdot 10^{-5}$	84/222	190	190

Table 1: Inputs for calculation of count rates in the different channels of interest for the polyethylene (CH₂) and carbon (C) targets for $\sqrt{s}=1.76$ GeV: reduction factors due to the combined acceptance and reconstruction efficiency (ε_{AR}), cross sections for π^-+p (σ_H) and π^-+C (σ_C) reactions, branching ratios (BR). The two last columns indicate the rate of reconstructed events per shift. For the polyethylene target, the first and second numbers corresponds to interactions with protons and to the total, respectively.

group, we expect to make a strong impact in the understanding of the light baryon spectrum in this energy interval.

Baryon-meson couplings

The two-pion channels with a cross section of the order of 6.5-10 mb can be measured with a very large statistics and will help to improve the PWA and scrutinize the role of the meson ρN channel. Resonant final states of the type $N(1440)\pi$, $N(1520)\pi$, \dots also attract much interest since they are related to the three body nature of baryonic resonances, which might be a dominant decay mode in the case of the unobserved (or "missing") resonances. The study of 2π production in photo and electro-production was also recently used to provide evidence for a new $N^*(1720) 3/2^+$ resonance [6], with a mass lower by 20 MeV than the known $N(1720)$ and with very different ρ and electromagnetic $3/2^+$ couplings. By providing complementary data from pion-induced reactions, our experiment can bring a timely contribution to this hadron structure highlight. The data for the ηn , $K\Lambda$ and $K\Sigma$ channels also need to be improved, which can in particular be used to firmly establish the existence of other resonances. Although high-precision differential spectra are largely lacking, the total cross sections for hadronic channels in π^-+p reactions within the 1.68 to 1.8 GeV range are generally known with a precision of 10-20%. The reconstruction efficiencies for exclusive channels can be estimated based on previous analyses of HADES data, such as [3] for charged double-pion production (see Table 1).

The reconstruction of the neutral hyperon production can be most efficiently achieved using the K_S^0 production corresponding to half of the cross section in the corresponding exclusive K^0 production channel. The missing mass resolution of $\sigma = 11$ MeV/ c^2 in the 2π decay channel, as measured in previous experiments, is sufficient to resolve the Λ and Σ^0 states. For the $\Sigma^- K^+$, an efficiency of 13% is estimated. For the η and ω production, we use the decay into $\pi^+ \pi^- \pi^0$, which can be reconstructed with efficiencies of 1% and 1.5% for η and ω , respectively, as deduced using simulations including the ECAL. The count rates for the carbon target need also to be determined, as they contribute to the statistical errors for the measurement of the π^-+p reaction obtained by subtraction of pion-carbon interactions from the polyethylene data. Reaction cross-sections measured for pion-nuclei reactions scale as $A^{2/3}$ [7]. However, for the production of pions, which undergo strong absorption already in carbon, we used a ratio $\sigma_C/\sigma_p = 1.6$ as measured at $\sqrt{s}=1.49$ GeV.

Hyperon production and polarization

In the 1970s a large transverse polarization of Λ hyperons has been discovered in unpolarized proton-beryllium collisions. Since then, similar polarization effects have been observed in various reactions, like e.g. lepton-hadron deep-inelastic scattering, hadron-hadron and hadron-nucleus collisions and electron-positron annihilation. A solid understanding of the mechanism causing alignment is still missing. Various theoretical model studies are successful in describing certain observations [8, 9], however, none of them is able to describe the world data in a consistent way. The nonzero recoil polarization is also observed for the Σ or Ξ hyperons.

More detailed studies of this phenomenon are crucial not only to boost the understanding of the strangeness production mechanism, but also to obtain fundamental information about the hyperon-nucleon (Y-N) interac-

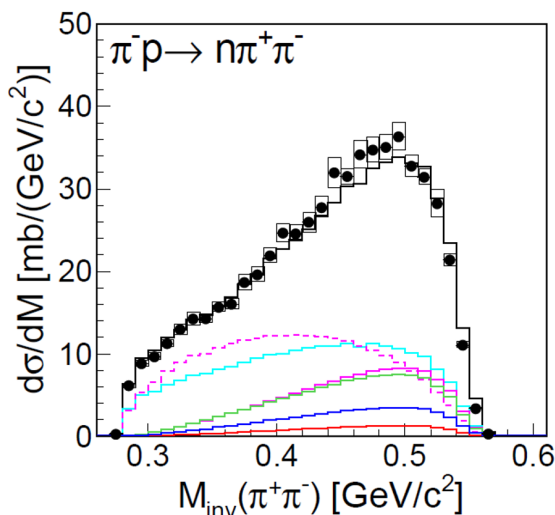


Figure 2: The $\pi^+\pi^-$ invariant mass distribution (black circles) measured with HADES in the $\pi^-p \rightarrow \pi^+\pi^-n$ reaction for a pion incident momentum of 0.685 GeV/c compared to the Bonn-Gatchina PWA solution (black solid line histogram), with the subdivision into the isobar $\Delta\pi$ (cyan), $N\sigma$ (dashed violet) and $N\rho$ (violet). The ρ contributions from s-channels (green curves) as well as from D13 (blue curve) and S11 (red curves) partial waves are also displayed.

tion or the nuclear force in general. These studies will also help to unravel the hyperon polarization observed in (ultra-)relativistic heavy-ion collisions (URHIC). Studies of the dynamics of URHIC using hydrodynamics revealed the occurrence of vorticity due to frictional forces. These turbulences in turn can cause an alignment of spins via equipartition of orbital rotation and spin due to local thermalization [10]. Hyperon (Λ , Σ^0) polarization data measured in pion beam experiments in the last century suffer from large statistical errors and also uncontrolled systematic errors. Precise measurements of the polarization strength in pion-induced strangeness production, and the identification of angular regions with the highest polarization, can be very useful for designing future measurements with secondary hyperon beams, like the J-PARC experiment [11]. J-PARC will use high intensity $\pi^{+/-}$ beams to perform precise N^* baryons spectroscopy and measurements of spin observables of the Λ -p scattering with a polarized Λ secondary beam.

The statistics obtained for the hyperon production will also suffice to address aspects of studies of CP violation. CP violation in the hyperon sector can be observed if there is interference between CP-even and CP-odd terms in the decay amplitude. A CP violation signal in the hyperon decays has been recently extracted in the BESIII and HyperCP experiments. The BESIII collaboration has developed a new and very sensitive method to study the CP violation effects using sequentially decaying entangled baryon-antibaryon pairs produced in the $e^+e^- \rightarrow J/\psi \rightarrow \Lambda\bar{\Lambda}/\Xi^-\bar{\Xi}^+$ processes [12]. Details of the measurement can be found in our white paper [13].

To gain direct and more precise information on the strong-phase difference and increase the sensitivity to CP violation effects, the knowledge on the $\Lambda - \pi^-$ final-state interaction (FSI), which enters the calculations, is needed. Such effect can be studied with the HADES detector and pion beams in the three-body $\pi^- + p \rightarrow \Lambda + \pi^- + K^+$ reaction. Using a partial wave or Dalitz plot analysis the $\Lambda - \pi^-$ FSI effects can be pin-down. These studies will be complementary to measurements planned at the JLab facility with photon beams.

Expected results

Building on the success of previous pion-beam measurements by the HADES collaboration in the second-resonance regime, we aim to acquire new and complementary precision data in the as-yet unexplored third resonance region. Our focus is on selective observables that are anticipated to have a significant impact on the field as outlined below.

Baryon-meson couplings

Using a PWA applied to the first pion-beam experiment taken in 2014 on the π^+ , π^- and π^0 channels, we were able to constrain the ρ production (Fig. 2) and to extract the branching ratios of the $N(1440)$, $N(1520)$ and $N(1535)$ baryon resonances to the ρN channel. Eight new entries have been added to the Review of Particle Physics for the branching ratios of $N^*(1520)$ and $N^*(1535)$ decays into $\Delta\pi$, $\rho\pi$, $N\sigma$ final states. The impact of HADES pion beam data for the structure of light baryons is acknowledged by the hadronic physics community

(see e.g. the recent review [14]). The new information on the ρN couplings in the second resonance region has then been used for the interpretation of the dielectron production, by means of the Vector Dominance Model.

We take these results as a proof of concept of the PWA method for HADES pion beam data in the two-pion production channels, which can be easily extended for other hadronic channels in the third resonance region. At a center-of-mass energy \sqrt{s} around 1.73 GeV, many hadronic channels are open (e.g. $K^0\Lambda$, $\Sigma^0 K^0$, $\Sigma^+ K^-$, ηn , ωn , ...) in addition to the two pion production. These channels will help to constrain hadronic couplings of baryon states in this region ($\Delta(1620) 1/2^-$, $\Delta(1700) 3/2^-$, $N(1650) 1/2^-$, $N(1675) 5/2^-$, $N(1680) 5/2^+$, $N(1710) 1/2^+$, $N(1720) 3/2^+$, ...) which are very poorly known. Our goal will therefore be to provide high statistics differential data for hadronic channels, including those with neutral mesons by use of the new Electromagnetic Calorimeter. These measurements will be included in a PWA, together with the very precise existing measurements in photo- and electroproduction reactions. In first place, the two-pion channels with a cross section of the order of 6.5-10 mb can be measured with a very large statistics and will provide new determinations to the $2\pi N$ channels, and especially to ρN which has a strong impact for medium effects, as mentioned above. Resonant final states of the type $N(1440)\pi$, $N(1520)\pi$, ... also attract much interest since they are related to the three body nature of baryonic resonances, which might be a dominant decay mode in the case of the unobserved (or "missing") resonances. The study of 2π production in photo and electro-production was also recently used to provide evidence for a new $N(1720) 3/2^+$ resonance [6], with a mass lower by 20 MeV and very different ρ and electromagnetic couplings with respect to the known $N(1720) 3/2^+$ resonance. By providing complementary data from pion induced reactions, our experiment can bring a timely contribution to this hadron structure highlight. The data base for the ηn , $K\Lambda$ and $K\Sigma$ channels also need to be improved. New pion beam data would nicely complement recent results obtained in photo and electroproduction experiments for these channels [14, 15], and help establishing the existence of other N^* or Δ resonances.

Although good precision differential spectra are badly missing, the total cross sections for hadronic channels in $\pi^- + p$ reactions in the region between 1.68 and 1.8 GeV are in general known with a precision of 10-20% and the reconstruction efficiencies of exclusive channels can be estimated based on previous analyses of HADES data, as [3] for the charged double pion production (see Table 1). The reconstruction of the neutral hyperon production can be most efficiently achieved using the K_S^0 production corresponding to half of the cross section in the corresponding exclusive K^0 production channel. The reconstruction of K_S^0 via their decay into $\pi^+\pi^-$ decay is used, with a branching ratio of 69% and an efficiency of $\varepsilon_{AR} = 4\%$, as deduced from full scale GEANT simulations, which were validated by previous reconstructions of K_S^0 in HADES experiments. The missing mass resolution of $\sigma = 11 \text{ MeV}/c^2$, as measured in previous experiments is then sufficient to resolve the Λ and Σ^0 states. For the $\Sigma^- K^+$, an efficiency of 13% is estimated. For the η and ω production, we use the decay into $\pi^+\pi^-\pi^0$, which can be reconstructed with efficiencies of 1 % and 1.5% for η and ω , respectively, as deduced using simulations including the ECAL.

The count rates for the carbon target need also to be determined, as they contribute to the statistical errors for the measurement of the $\pi^- + p$ reaction obtained by subtraction of pion-carbon interactions from the polyethylene data. Hadronic channels in π -A reactions are also interesting by themselves, for cold matter studies, as developed further below. We therefore give count rates for measurements on the carbon and silver targets for the above-mentioned channels. Inclusive meson production will be measured with even higher yields. Reaction cross-sections measured for pion-nuclei reactions scale as $A^{2/3}$ [7]. However, for the production of pions, which undergo strong absorption already in carbon, we used a ratio $\sigma_C/\sigma_p = 1.6$ as measured at $\sqrt{s}=1.49 \text{ GeV}$. For the exclusive strangeness production channels, we neglect the absorption and deduce the cross sections for the reaction on carbon and using the relation $\sigma \sim Z^{2/3}$, as mainly protons are involved.

Experimental set-up

We describe here only changes relative to the beam time taken in 2022. The forward detectors (**FD**), including the straw tracking stations and the forward RPC, will not be used for this run. The **ECAL** has now all six sectors equipped and provides independent measurement of neutral meson production. A **T0** detector based on Low Gain Avalanche Diode or on scCVD diamond technology will be installed in front of the HADES target with similar geometries as used in 2014. The **MDC** will be operated with the new front-end electronics providing multi-hit capability and a reduced dead time.

The secondary pion beam is produced using an extracted primary ^{14}N beam at the highest possible intensity

impinging on a 10 cm long beryllium target. In a test beam time conducted by Accelerator division it was demonstrated, that a ^{14}N beam of 7×10^7 ions per spill and at maximum rigidity could be slow-extracted to the pion production target without surpassing safety radiation levels. The spill length will be set such as to not go below a duty cycle of 50%. The exact value will depend on the spill shape and on the fill and acceleration time. Comparing to the performance in 2014, we expect about 800.000 π^- per spill impinging on our target.

Justification of the beam time

To ideally cover the third resonance region, we propose to perform an energy scan consisting of five bins centered at $\sqrt{s}=1.67$ GeV ($p_\pi = 1.007$ GeV/ c), $\sqrt{s}=1.70$ GeV ($p_\pi = 1.061$ GeV/ c), $\sqrt{s}=1.73$ GeV ($p_\pi = 1.115$ GeV/ c), $\sqrt{s}=1.76$ GeV ($p_\pi = 1.171$ GeV/ c) and $\sqrt{s}=1.79$ GeV ($p_\pi = 1.228$ GeV/ c). We reach good sensitivity for the different key measurements discussed above with a total of **66** shifts, according to the following configuration:

- ▶ 7 shifts for each of the five energies on the polyethylene target and 5.5 shifts on the carbon target for each setting.
- ▶ 3.5 shifts for tuning and calibration. In particular, the alignment of the primary beam on the pion production target and of the pion beam on the t0 detector in front of the target needs careful adjustments of the corresponding dipoles.

$\pi^+\pi^-n$	$\pi^0\pi^-p$	$\pi^0\pi^0n$	$K^0\Lambda$	Σ^0K^0	Σ^-K^+	ηn	ωn
24×10^6	10×10^6	3.4×10^5	1.3×10^5	5.6×10^4	5.0×10^5	8.4×10^4	3.4×10^5

Table 2: Average statistics expected for hadronic final states in the $\pi^- + p$ reaction around $\sqrt{s}=1.73$ GeV for 7 shifts on the polyethylene target.

As deduced from the analysis of the 2014 experiment, the PWA requires a statistics of about 10^5 events for accurate results from PWA in the charged $2\pi N$ channels and of 10^4 for the two-body channels. Our estimates shown in Table 2 (based on Tab. 1 show that, for the channel $\Sigma^0 K^0$, which has the smallest yield, this goal can be obtained for each setting with 7 shifts on the CH_2 target, as shown in Table 1. In addition to the channels listed in Table 2 the Λ polarization will be measured. For Λ the polarization will be obtained for each energy point with the estimated statistical accuracy of 5 – 8%. We need in addition 5.5 shifts per energy point for the accurate subtraction of interactions with carbon nuclei in the polyethylene target. To do so, the characteristics of events measured in polyethylene and carbon targets will be compared by means of a χ^2 test, a method which has been validated in the previous experiment [3]. In this way, we can have a collection of high statistics differential cross sections for various hadronic channels which will be very valuable for the PWA.

Bibliography

- [1] W. J. Briscoe et al. Physics opportunities with meson beams. *Eur. Phys. J.*, A51(10):129, 2015.
- [2] J. Adamczewski-Musch et al. Probing dense baryon-rich matter with virtual photons. *Nature Phys.*, 15(10):1040–1045, 2019.
- [3] J. Adamczewski-Musch et al. Two-pion production in the second resonance region in π^-p collisions with the High-Acceptance Di-Electron Spectrometer (HADES). *Phys. Rev. C*, 102(2):024001, 2020.
- [4] R. Abou Yassine et al. Inclusive e^+e^- production in collisions of pions with protons and nuclei in the second resonance region of baryons. *acc. by PRC*, arXiv:2309.13357, 2023.
- [5] R. Abou Yassine et al. First measurement of massive virtual photon emission from n^* baryon resonances. *sub. to PRL*, arXiv:2205.15914, 2024.
- [6] V. I. Moiseev et al. Evidence for the $N'(1720)3/2^+$ Nucleon Resonance from Combined Studies of CLAS $\pi^+\pi^-p$ Photo- and Electroproduction Data. *Phys. Lett.*, B805:135457, 2020.
- [7] B. W. Allardyce et al. Pion reaction cross-sections and nuclear sizes. *Nucl. Phys.*, A209:1–51, 1973.
- [8] T. A. DeGrand and H. I. Miettinen. . *Phys. Rev.*, D23:1227, 1981.
- [9] T. A. DeGrand and H. I. Miettinen. . *Phys. Rev.*, D24:2419, 1985.
- [10] F. Becattini, V. Chandra, L. Del Zanna, and E. Grossi. Relativistic distribution function for particles with spin at local thermodynamical equilibrium. *Annals Phys.*, 338:32–49, 2013.
- [11] K. H. Hicks and H. Sako. J-PARC Proposal E45, Japan, 2012; <http://www.phy.ohiou.edu/~hicks/NSF/2013/JPARC-P45.pdf>.
- [12] Elisabetta Perotti, Göran Fäldt, Andrzej Kupsc, Stefan Leupold, and Jiao Jiao Song. Polarization observables in e^+e^- annihilation to a baryon-antibaryon pair. *Phys. Rev. D*, 99(5):056008, 2019.
- [13] HADES Collaboration. π -QCD - proposal for experiments at the gsi pion beam facility. https://hades.gsi.de/sites/default/files/web/media/documents/proposals/HADES_Proposal_Pion_TitlePage-only.pdf.
- [14] Annika Thiel, Farah Afzal, and Yannick Wunderlich. Light Baryon Spectroscopy. *Prog. Part. Nucl. Phys.*, 125:103949, 2022.
- [15] D. S. Carman et al. Beam-Recoil Transferred Polarization in K^+Y Electroproduction in the Nucleon Resonance Region with CLAS12. *Phys. Rev. C*, 105:065201, 2022.

7 Letters of support

Expression of Interest: Hypernuclei Measurements in Pion-Induced Reactions on Nuclear Targets with HADES

Hypernuclei, exotic nuclei containing one or more hyperons, represent a critical area of study in nuclear and particle physics. They provide unique insights into the strong interaction under extreme conditions and help bridge our understanding between conventional nuclear matter and the strange quark sector. Hypernuclei studies are also essential for understanding astrophysical phenomena, such as the structure and stability of neutron stars, where hyperons are expected to play a significant role in their dense cores. Precise measurements of hypernuclei lifetimes, binding energies, and decay channels can refine theoretical models of hyperon-nucleon and hyperon-hyperon interactions.

Pion-induced reactions offer unique advantages for hypernuclei production due to the low recoil momentum of the secondary particles. These recoil-less kinematics increase the probability of hypernuclei formation, providing an efficient mechanism for their study. The small recoil momentum allows for extended interaction times within the nuclear medium, facilitating the formation and stability of hypernuclei.

The High Acceptance Di-Electron Spectrometer (HADES) is uniquely positioned to explore hypernuclei in pion-induced reactions. Its particle identification (PID) and vertex reconstruction capabilities, combined with advanced data analysis techniques such as artificial neural networks (ANNs), enable the precise reconstruction of hypernuclei and accurate measurements of their lifetimes and branching ratios. This makes HADES an excellent platform for hypernuclear research.

The proposed measurements on cold nuclear matter aim to leverage significant improvements in the pion beam properties and detector technologies compared to the 2014 experiment. Hence, the anticipated beamtime in 2026 offers substantial enhancements over the 2014 experiment leading to an overall gain factor of 90. This significant increase in efficiency and data collection capability translates into an expected production of approximately: 10000 hypernuclei

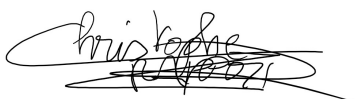
These yields represent an up to now unmatched amount, (almost an order of magnitude increase) of hypernuclei statistics at GSI and will enable statistically robust studies of hypernuclei properties, including lifetimes, branching ratios, and formation dynamics.

Conclusion

The combination of improved pion beam characteristics, upgraded detector capabilities, and HADES's proven expertise in hypernuclei research makes the proposed measurements a unique opportunity to advance our understanding of hypernuclei and cold nuclear matter. The high precision and expected yields will provide unparalleled insights into hypernuclear structure and the role of hyperons in dense matter.

We strongly express our interest in conducting these hypernuclei measurements within the HADES experimental framework. The proposed experiments will not only complement existing studies but also pave the way for future high-precision investigations at FAIR and other facilities.

Christophe Rappold
Instituto de Estructura de la Materia – CSIC
Serrano 121, ES-28006 Madrid



Baryon spectroscopy with a π^- -beam at HADES

To understand the complex bound states of Quantum Chromodynamics is one of the key challenges in hadron and particle physics. Significant progress in the understanding of the light baryon spectrum, made up of u- and d-quarks, has been made in recent years dominantly based on the high quality photoproduction data becoming available from ELSA, JLab, MAMI and other facilities worldwide. The number of well know states considered in the summary tables of the Review of Particle Physics has increased by about 40% since 2010 and a large number of formerly unknown properties of the states has been determined.

Nevertheless the light baryons cannot yet be considered understood and new questions did arise based on the new results. E.g. still not all states expected by constituent quark models, have been identified. Do they exist? In addition, the baryons observed show a mass pattern which is neither expected by quark models nor by present lattice QCD calculations: many states, even though not all of them, seem to have parity partners - a state close in mass with opposite parity. In addition, in the strange baryon sector, there are indications for the $\Lambda(1405)$ being a 2-pole-structure. Two low mass isoscalar $1/2^-$ -states in this sector are at clear variance with quark model expectations. The possible existence of states of molecular nature in the spectrum of baryons is not only very interesting but it also makes the spectrum of baryons even more complex and more difficult to understand.

From the experimental side, new data - photoproduction data (polarization observables and data off the neutron) but also data taken with different probes (πN) - are of large importance to finally pin down the spectrum and properties of baryon resonances in the light quark (u,d,s) sector. Only based on new data, we will finally be able to understand the observations mentioned above or to answer questions such as whether e.g. the states belonging to the $SU(6)\times O(3)$ -20'plet exist, or whether the strange baryons, presently very badly known, fit to the N^* - and Δ^* - states observed (multiplet structures).

Here, new high quality HADES data on πN -scattering can make an important impact. Adding new πN -scattering data into the data base of coupled channel partial wave analyses (PWA), such as the Bonn-Gatchina PWA, used to extract the resonances from the data is of large interest. Without doubt high quality inelastic πN -scattering data will provide important constraints to the fits beyond the data presently available.

In the present coupled channel fits of photoproduction data, state-of-the-art PWAs, such as e.g. the Jülich-Bonn dynamical coupled channel analysis or the Bonn-Gatchina partial wave analysis do also include pion-nucleon (elastic) scattering data. Obviously the πN -elastic partial waves provide important constraints related to the πN -couplings of resonances.

Unfortunately for most πN inelastic channels, like e.g. $\pi^- p \rightarrow \eta p$, the quality of existing data is clearly insufficient. Here new HADES data can substantially improve the situation and make a huge impact.

Let me use $\pi^- p \rightarrow p\eta$ as an example where new HADES data is of large interest for the PWA. The surprising decay pattern of the two lowest-mass nucleon excitations, $N(1535)\frac{1}{2}^-$ and $N(1650)\frac{1}{2}^-$ into $p\eta$ has always been a challenge to understand. In 2010, the $N\eta$ branching ratio of $N(1535)\frac{1}{2}^-$ was estimated by the PDG to be 45-60%, and only 3-10% for $N(1650)\frac{1}{2}^-$. This puzzling difference led to quite different and in part exotic explanations for $N(1535)\frac{1}{2}^-$: e.g. large pentaquark components in the $N(1535)\frac{1}{2}^-$ wave function have been suggested^a, or an explanation of the state as dynamically generated $K\Sigma$ - $K\Lambda$ bound-state decaying strongly into $p\eta$ via coupled-channel effects was given^b. Based on the recent high quality photoproduction data taken with polarized target and polarized beam the situation has changed substantially^c. The puzzling difference in the $p\eta$ branching ratio almost disappeared. Within the BnGa-PWA we find $p\eta$ branching ratios for the lower and higher mass $\frac{1}{2}^-$ -resonance of 0.41 ± 0.04 and 0.33 ± 0.04 respectively^c. New data on $\pi^- p \rightarrow \eta p$, sensitive to the πN and ηN couplings of the states is highly welcome. A PWA including the photoproduction data and at the same time the πN elastic and inelastic data within a coupled channel framework would be extremely powerful. The pole positions and couplings of the resonances are of course the same in all the reactions. Fitting $\gamma p \rightarrow p\pi^0$ and $\gamma p \rightarrow p\eta$ (differential cross sections and polarization observables) together with $\pi^- p \rightarrow \eta p$ and the elastic πN partial waves would constrain the couplings in an optimal way. It can be expected that this controversially discussed issue would be finally settled after the respective coupled channel PWA has been performed.

A nice example for such a combined analysis of HADES and photoproduction data which was already performed within the BnGa-PWA framework is the analysis of the HADES $\pi^- p \rightarrow \pi^+ \pi^- n$ - and $\pi^- p \rightarrow \pi^0 \pi^- p$ -data in the second resonance region^d. The different charged two-pion modes measured by HADES provided important constraints for the determination of the $\Delta\pi$, $N\sigma$, and especially $N\rho$ decay modes of the contributing states. This analysis did not only result in 8 new entries in the Review of Particle Physics for $N(1520)3/2^-$ and $N(1535)1/2^-$ but it was also important for the understanding of effective electromagnetic baryon transition form factors^e and to reach a better understanding of dielectron production in the second resonance region.

^aB. S. Zou, EPJA 35 (2008) 325.

^bN. Kaiser, et al., PLB 362 (1995) 23., M. Mai, P.C. Bruns, U.-G. Meissner, PRD 86 (2012) 094033.

^cJ. Müller et al. [CBELSA/TAPS], PLB 803 (2020) 135323

^dJ. Adamczewski-Musch et al. [HADES], PRC 102, 024001 (2020)

^eR. Abou Yassine et al. [HADES], arXiv:2205.15914 [nucl-ex]

Needless to say that such combined fits of high statistics photoproduction data (existing and to come) providing also polarization degrees of freedom together with π^-p -scattering data from HADES will be of advantage with regard to many final states.

This includes final states without and with strangeness. The latter having the advantage that the weak decay provides in addition access to the recoil polarization. As mentioned above, even though important for our understanding of the baryons as QCD bound states, data on strange baryons is very scarce. Here the established resonances remained the same for more than 30 years and progress is hampered by the lack of data. The only interesting exception is the 2-pole structure of the $\Lambda(1405)$ mentioned above. Also here using different probes will be of large interest to gain a comprehensive picture on the Λ^* - and Σ^* -resonances. The contributing background amplitudes and sensitivities will be different in πN and γN providing thus complementary information for the PWA. Here in a first step, the first excitation band, well studied in the non-strange sector, needs to be understood.

Before I close, I cannot resist mentioning that the use of a π^+ -beam, if possible, would also make an important impact in studies of the production of Δ^* -resonances avoiding contributions from N^* -resonances and thus simplifying the PWA.

Kind regards,

(Ulrike Thoma)

Neutrino oscillation physics is entering the era of high precision measurements. The next generation experiments that are under construction (Hyper-Kamiokande, DUNE) will improve significantly the statistics with respect to the currently running projects such as T2K and NOvA and hopefully will be able to answer the question about CP symmetry violation in the neutrino sector. The strategy of the measurement in the accelerator neutrino oscillation experiments heavily relies on the precise modeling of the near and far detectors, neutrino flux and neutrino interactions. The most challenging aspect to manage in this framework is related to the modeling of neutrino interactions. The accelerator neutrino experiments use nuclear targets in order to increase the number of observed neutrino interactions. This fact has also negative implications because the neutrino interactions with nuclei are far more complicated than the relatively well-known neutrino-nucleon reactions. The experiments can only measure the neutrino cross sections for ‘observed’ reactions that are based on the number of particles that leave the nucleus after interaction and the properties of these particles. The nuclear effects smear the entire picture because the primary pions and nucleons can re-interact before they leave the nucleus. These re-interactions are known as Final State Interactions (FSI) and cannot be directly measured, thus the accelerator neutrino experiments rely on proper modeling of FSI based on external measurements (e.g. from experiments studying pions interactions). The smearing due to the FSI is particularly affecting the neutrino energy reconstruction because in the accelerator neutrino experiments it relies on properly reconstructed kinematics and the multiplicities of the particles in the final state of neutrino interaction. Monte Carlo simulations attempt to correct for effects such as FSI by tuning the cross sections from dedicated pion/proton-nucleus cross-section measurements. The access to the new pion-nucleus cross-section measurements is crucial to improve the precision of the neutrino oscillation measurements in present and future long-baseline experiments. The data from pion-nucleus scattering experiments will help to tune the models of pion re-scattering in the nucleus. The momentum of pions exiting the nucleus after neutrino-nucleus interaction depends on the energy of the primary neutrino. Typically, for T2K and Hyper Kamiokande the momentum of pions has a peak around 200 MeV and extends up to 1 GeV with the most desirable targets for pion scattering such as: H₂O, CH, Ar, Fe, Pb (near and far detector components). We express our support for the plan of performing pion scattering cross-section measurements in the conditions mentioned above.

Sincerely,

Tomasz Wąchała (T2K, IFJ PAN)

Grzegorz Żarnecki (T2K, IFJ PAN)

The neutrino long-baseline oscillation experiments are entering into the precision era, with the currently running experiments (T2K and NOVA) and with the next generation of experiments now under construction (HyperKamiokande and DUNE) which will enable an increase of a factor 100 in statistics with the respect to present measurements.

The main challenge to high precision oscillation measurements consists in precisely controlling the systematic uncertainties on the total rate of produced neutrinos (flux), the rate of neutrino-nucleus interactions in the detectors (cross-section and detector efficiency) and the reconstruction of neutrino energy from the outgoing particles of the interactions (nuclear effects in cross-section and detector calibration). The strategy of long-baseline experiments consists in relying on a highly capable set of near detectors for controlling uncertainties on cross-section and flux. While such strategy is particularly effective, notably for the control of the rate, there are nuclear effects related with the initial state of nucleons in the nucleus and with the final state re-interactions of produced particles in the nucleus, which are not directly accessible in an unambiguous way with near detector measurements. Long-baseline experiments therefore rely also on external measurements (i.e. measurements performed from other, dedicated experiments) for the control of such nuclear effects.

A particularly relevant case is the re-interaction of hadrons (pions and nucleons) produced in the neutrino interactions inside the nuclear matter. Such re-interactions could change the kinematics, multiplicity and charge of the outgoing hadrons, thus affecting the neutrino energy reconstruction. To correct for such effects, the simulation incorporates cross-section tuning from dedicated pion-nucleus (and proton-nucleus) cross-section measurements. The most recent work in this direction is published in (Phys.Rev.D 99 (2019) 5, 052007), which relies on a quite limited set of previously available pion scattering data. A very important part which is still missing in this approach, consists in the tuning of the outgoing pion kinematics from pion-nucleus re-interactions: up to now, the simulation only incorporate external constraints on the total pion cross-section rate (by interaction channel) but we do not use yet 'differential' measurements to further tune the kinematics of the outgoing pions. This further step is becoming crucial since, to have precise enough neutrino energy reconstruction, we are starting to use/analyse all the particles in the final state (not only leptons, as in the past, but also pions and nucleons)

The availability of new pion-nucleus cross-section measurements, notably if differential in the outgoing pion kinematics, is therefore of crucial importance to improve the precision of the neutrino oscillation measurements in present and future long-baseline experiments. Such measurements will help to tune directly the models of pion re-scattering in the nucleus and, indirectly, the models of nucleon-rescattering in the nucleus.

The typical momentum of pions (and nucleons) produced in neutrino-nucleus interactions depends (only slightly) on the energy of the initial neutrinos (<1 GeV for T2K and HyperKamiokande, <5 GeV for DUNE) and on the dynamics of the neutrino interaction itself (transferred energy from the neutrinos to the nucleus). Indeed, we work mostly in the region of Delta resonances where the cross-section is saturated, thus the momentum of pions which are produced in neutrino interactions are quite similar between HyperKamiokande and DUNE. The momentum of pions escaping the nucleus has a peak around 200MeV and a tail which goes up to 1 GeV for HyperKamiokande and 1.5 GeV for DUNE. (Nucleons escaping the nucleus are typically peaked at a momentum around 500 MeV). I understand that such low momenta are difficult to perform for the pion beam in HADES, but probing the nuclear physics models even at slightly larger energy could still be useful to tune them properly.

Near and far detectors feature different target nuclei, depending on the experiment, (notably H_2O , CH , Ar) but to ensure proper control of nuclear modeling, data from a

variety of different nuclei is useful (as demonstrated in the paper above).

Technological prototypes of near and far detectors (eg, protoDUNE) has been exposed to test beams (including pion beams) to measure pion-nucleus cross-section but the precision achievable is limited by the fact that such detector are not designed for this specific use case and thus the precision they can reach is limited.

Sara Bolognesi
(IRFU/Saclay, T2K+DUNE)

8 The HADES Collaboration

R. Abou Yassine^{6,14}, J. Adamczewski-Musch⁵, T. Aumann⁶, M. Becker¹⁰, A. Blanco¹, C. Blume⁸, M. Bohman¹⁶, A. Bronis¹³, P. Chudoba^{15,f}, I. Ciepał³, S. Deb¹⁴, M. Duer⁶, R. Dvorak^{15,f}, M. Durr¹⁰, L. Fabbietti⁹, M. Firlej², T. Fiutowski², H. Floersheimer⁶, A. Foda⁵, P. Fonte^{1,a}, J. Friese⁹, I. Fröhlich⁸, J. Fortsch¹⁹, T. Galatyuk^{6,5,c}, R. Gernhäuser⁹, M. Grunwald¹⁸, D. Grzonka⁵, M. Gumberidze⁵, S. Harabasz^{6,c}, T. Heinz⁵, C. Höhne^{10,5}, R. Holzmann⁵, M. Idzik², L. Ji⁶, B. Kämpfer^{7,d}, K-H. Kampert¹⁹, B. Kardan^{8,e}, V. Kedych⁶, S. Kim¹⁹, V. Kladov⁵, R. Kliemt⁵, I. Koenig⁵, W. Koenig⁵, M. Kohls^{8,e}, P. Kohout^{13,15}, A. Kohoutova^{13,15}, J. Kolas¹⁸, J. Kollarczyk^{15,f}, G. Korcyl⁴, G. Kornakov¹⁸, W. Krueger⁶, L. Krupa¹³, A. Kugler¹⁵, M. Kurach¹⁸, R. Lalik⁴, T. Leontiou¹², S. Linev⁵, F. Linz^{6,5}, L. Lopes¹, M. Lorenz⁸, P. Marciniowski¹⁶, J. Markert⁵, T. Matulewicz¹⁷, J.G. Messchendorp⁵, V. Metag¹⁰, J. Michel⁸, A. Molenda², J. Moron², J. Mousa¹², C. Müntz⁸, M. Nastroth⁸, A. Obertelli⁶, D. Okropiridze⁵, A. Opichal^{15,13}, J. Orliński¹⁷, M. Papenbrock¹⁶, Y. Parpottas¹², M. Parschau⁸, S. Pattnaik⁵, C. Pauly¹⁹, D. Pawlowska-Szymanska¹⁸, V. Pechenov⁵, O. Pechenova⁵, G. Perez Andrade⁵, D. Pfeifer¹⁹, K. Piasecki¹⁷, J. Pietraszko⁵, A. Podwyszocka¹⁷, T. Povar¹⁹, M. Predota¹⁸, K. Prościński^{4,b}, W. Przygoda⁴, B. Ramstein¹⁴, N. Rathod¹⁸, J.T. Rieger¹⁶, J. Ritman⁵, A. Rost^{6,5}, A. Rustamov⁵, S. Sahu⁵, P. Salabura⁴, J. Saraiva¹, S. Schadmand⁵, K. Scharmann¹⁰, N. Schild⁶, E. Schwab⁵, K. Schonning¹⁶, F. Seck⁶, I. Selyuzhenkov⁵, U. Singh⁴, L. Skorpil⁸, J. Smyrski⁴, S. Spies⁸, H. Ströbele⁸, J. Stroth^{8,5,e}, K. Sumara⁴, O. Svoboda¹⁵, K. Swientek², J. Taylor⁵, P. Thusty¹⁵, M. Traxler⁵, S. Trelinski³, H. Tsertos¹², I. C. Udea^{6,5}, F. Ulrich-Pur⁵, S. Velardita⁶, V. Wagner¹⁵, A.A. Weber¹⁰, C. Wendisch⁵, P. Wintz¹¹, A. Władyszewska^{4,b}, B. Włoch³, H.P. Zbroszczyk¹⁸, M. Zieliński⁴, P. Zumbach⁵

¹LIP-Laboratório de Instrumentação e Física Experimental de Partículas, 3004-516 Coimbra, Portugal

²AGH University of Krakow, Faculty of Physics and Applied Computer Science, 30-059 Krakow, Poland

³Institute of Nuclear Physics, Polish Academy of Sciences, 31342 Kraków, Poland

⁴Smoluchowski Institute of Physics, Jagiellonian University of Cracow, 30-059 Kraków, Poland

⁵GSI Helmholtzzentrum für Schwerionenforschung GmbH, 64291 Darmstadt, Germany

⁶Institut für Kernphysik, Technische Universität Darmstadt, 64289 Darmstadt, Germany

⁷Institut für Strahlenphysik, Helmholtz-Zentrum Dresden-Rossendorf, 01314 Dresden, Germany

⁸Institut für Kernphysik, Goethe-Universität, 60438 Frankfurt, Germany

⁹Physik Department E62, Technische Universität München, 85748 Garching, Germany

¹⁰II.Physikalisches Institut, Justus Liebig Universität Giessen, 35392 Giessen, Germany

¹¹Forschungszentrum Juelich, 52428 Juelich, Germany

¹²Department of Mechanical Engineering, Frederick University, 1036 Nicosia, Cyprus

¹³Univerzita Palackeho v Olomouci, 779 00 Olomouc, Czech Republic

¹⁴Laboratoire de Physique des 2 infinis Irene Joliot-Curie, Universite Paris-Saclay, CNRS-IN2P3, F-91405 Orsay, France

¹⁵Nuclear Physics Institute, The Czech Academy of Sciences, 25068 Rez, Czech Republic

¹⁶Institutionen for fysik och astronomi, Uppsala universitet, 75120 Uppsala, Sweden

¹⁷Uniwersytet Warszawski, Instytut Fizyki Doświadczalnej, 02-093 Warszawa, Poland

¹⁸Warsaw University of Technology, Faculty of Physics, 00-662 Warsaw, Poland

¹⁹Bergische Universität Wuppertal, 42119 Wuppertal, Germany

^a also at Instituto Politécnico de Coimbra, Instituto Superior de Engenharia de Coimbra,
3030-199 Coimbra, Portugal

^b also at Doctoral School of Exact and Natural Sciences, Jagiellonian University, Cracow,
Poland

^c also at Helmholtz Research Academy Hesse for FAIR (HFHF), Campus Darmstadt,
64390 Darmstadt, Germany

^d also at Technische Universität Dresden, 01062 Dresden, Germany

^e also at Helmholtz Research Academy Hesse for FAIR (HFHF), Campus Frankfurt,
60438 Frankfurt am Main, Germany

^f also at Czech Technical University in Prague, 16000 Prague, Czech Republic